

Chapter 8

Electrospun PVdF and PVdF-co-HFP-Based Blend Polymer Electrolytes for Lithium Ion Batteries



N. S. Jishnu, S. K. Vineeth, Akhila Das, Neethu T. M. Balakrishnan, Anjumole P. Thomas, M. J. Jabeen Fatima, Jou-Hyeon Ahn, and Raghavan Prasanth

8.1 Introduction

Advancement in technology has been in a booming rate with proliferation in population, which has adversely affected the rapid depletion of fossil fuels. Serious environmental issues related on overexploitation of these nonrenewable resources led to greenhouse effect, ozone layer depletion, global warming and climate changes. In addition to the above environmental issues, energy crisis is a serious issue. The post-fossil fuel era hence needs to find alternative source of energy. Sustainable and renewable energy source need to be explored to satisfy the exponentially increasing demand of energy. The effective utilization of energy from the renewable resources such as water (hydropower and hydrokinetic), wind, solar (power and hot water), biomass (biofuel and biopower), geothermal (power and heating) are the current possible solution. Globally, renewables made up 24% of electricity generation in 2014, in which the major contribution from hydropower (17%). Renewable energy is the fastest-growing energy source in the USA, increasing 67% from 2000 to

N. S. Jishnu
Rubber Technology Centre, Indian Institute of Technology-Kharagpur (IIT-KGP), Kharagpur,
West Bengal 721302, India

S. K. Vineeth
Department of Polymer and Surface Engineering, Institute of Chemical Technology, Nathalal
Parekh Marg, Matunga, Mumbai 400019, India

A. Das · N. T. M. Balakrishnan · A. P. Thomas · M. J. Jabeen Fatima · R. Prasanth (✉)
Department of Polymer Science and Rubber Technology, Cochin University of Science and
Technology (CUSAT), Cochin 682022, India
e-mail: prasanth@cusat.ac.in

J.-H. Ahn (✉) · R. Prasanth
Department of Materials Engineering and Convergence Technology, Gyeongsang National
University, 501 Jinju-Daero, Jinju 52828, Republic of Korea
e-mail: jhahn@gnu.ac.kr

© Springer Nature Singapore Pte Ltd. 2021

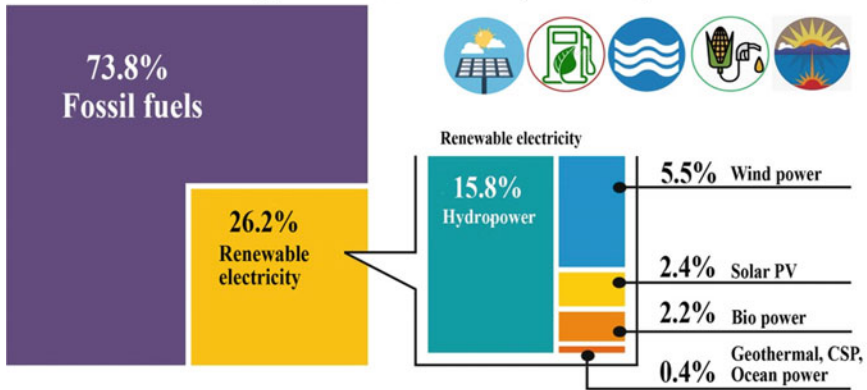
N. T. M. Balakrishnan and R. Prasanth (eds.), *Electrospinning for Advanced Energy Storage Applications*, Materials Horizons: From Nature to Nanomaterials,
https://doi.org/10.1007/978-981-15-8844-0_8

201

2016. Renewables made up 24% of global electricity generation in 2014, and that is expected to rise to 31% by 2040. Most of the increase will likely come from wind energy and hydropower. The estimated global renewable energy share of total final energy consumption in 2015 is shown in Fig. 8.1, and renewable energy indicator in 2016 is shown in Table 8.1

In this aspect, for the efficient storage and effective utilization of renewable energy required advanced high power energy storage devices. Among the different types of energy storage devices such as supercapacitors, batteries and fuel cells, the possibilities provided by the batteries are significant due to their high energy density, power density, easy to fabricate and portability. Compared to any other battery technology such as nickel–cadmium or nickel–metal halide batteries, etc., lithium-ion batteries are promising due to their superior energy density, output voltage, long cycle life

Estimated Renewable Energy Share of Global Electricity Production, End 2018



Estimated Renewable Energy Share of Total Final Energy Consumption, 2017

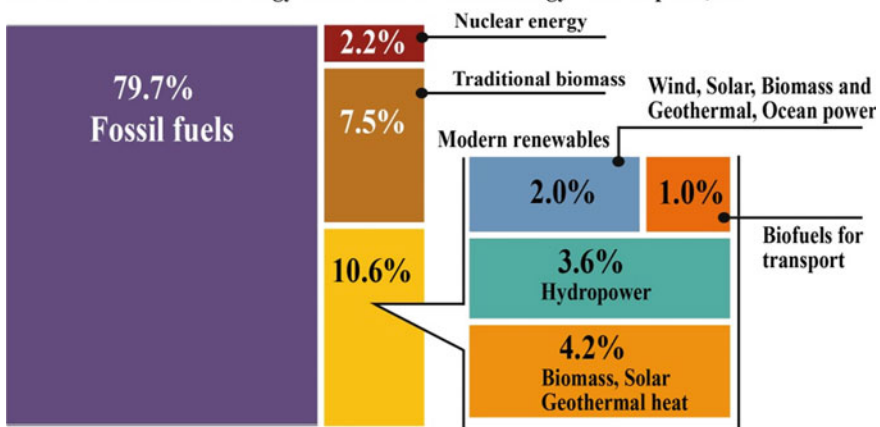


Fig. 8.1 Global renewable energy share of total final energy consumption in 2015

Table 8.1 Estimated global renewable energy share of total final energy consumption (2015)

		2015	2016
<i>Investment</i>			
New investment (annual) in renewable power and fuel	Billion USD	312.2	241.6
<i>Power</i>			
Renewable power capacity (total, not including hydro)	GW	785	921
Renewable power capacity (total, including hydro)	GW	1856	2017
Hydropower capacity	GW	1071	1096
Biopower capacity	GW	106	112
Biopower generation (annual)	TWh	464	504
Geothermal power capacity	GW	12	13.5
Solar PV capacity	GW	228	303
Concentrating solar thermal power capacity	GW	4.7	4.8
Wind power capacity	GW	433	487
<i>Heat</i>			
Solar hot water capacity	GW _{th}	435	456
Transport	GW		
Ethanol production (annual)	GW	98.3	98.6
Biodiesel production (annual)	GW	30.1	30.8

and electrochemical properties. The energy density of LIBs (250 Wh kg^{-1} , 650 Wh L^{-1}) is typically twice that of the standard nickel–cadmium batteries, and there is potential for higher energy densities. The load characteristics are reasonably good and behave similarly to nickel–cadmium in terms of discharge. The high cell voltage of 3.6 V allows battery pack designs with only one cell. Most of today’s mobile phones run on a single cell, while nickel-based pack would require three 1.2 V cells connected in series. Also LIBs is a low maintenance battery, an advantage that most other chemistries cannot claim. There is no memory, and no scheduled cycling is required to prolong the cycle life of the battery. In addition, the self-discharge is less than half compared to nickel–cadmium, making lithium ion well suited for modern fuel gauge applications [1]. Lithium-ion batteries (LIBs) were first commercialized by Sony Corporation in 1991, and this year, 2019, the Nobel Prize in Chemistry is awarded to John B Goodenough, M. Stanley Wittingham and Akira Yoshino “for the development of lithium-ion batteries” (Fig. 8.2).

Last two decades witnessed significant development of LIBs as its demand reflected in portable electronic gadgets, computers and related devices, and hybrid electric vehicles. Furthermore, the global market of lithium-ion batteries is currently growing, and it is expected that in 2022, the market value will reach \$ 46.21 billion, with an annual growth rate of 10.8%. The major components of a battery are anode (negative electrode, where reduction occurs), cathode (positive electrode, where oxidation occurs) and electrolytes. For the development of high energy density

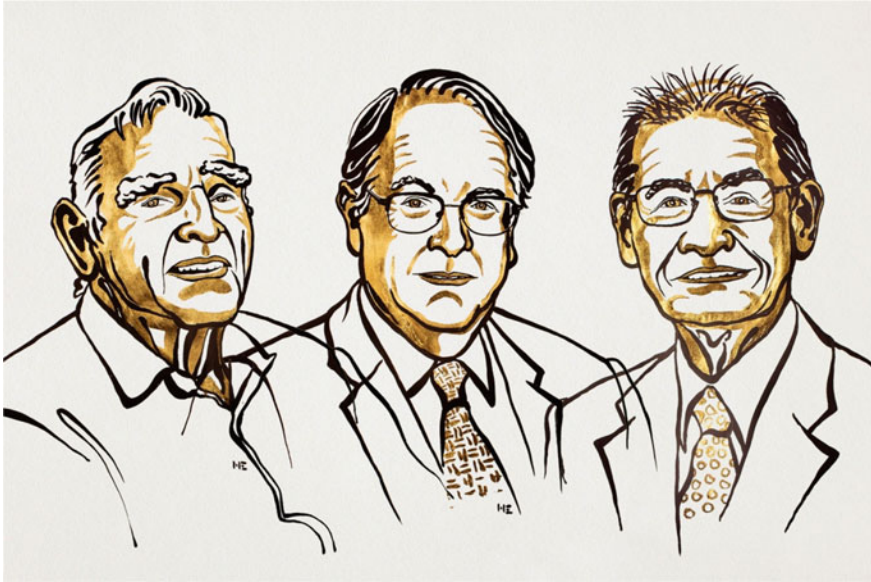


Fig. 8.2 Images of Nobel laureates 2019 (From right to left—John. B. Goodenough, Stanley M. Wittingham, Akira Yoshino) Adapted and reproduced from Ref. [2]. Copyright © Nobel Media 2019. Illustration: Niklas Elmehed

battery having improved safety, the major role played by the electrolyte, in which the conventional liquid electrolyte, is replaced with gel electrolyte as it have no leakage, good ionic conductivity and good dimensional stability. The gel electrolyte is a heterogeneous system in which a microporous polymeric membrane having more than 40% porosity is activated with a liquid electrolyte (typically 1 M solution) prepared by dissolving suitable lithium salt (LiPF_6 , LiClO_4 , LiTFSI , LiBOB) in a polar (propylene carbonate) or nonpolar (ethylene carbonate (EC), diethyl carbonate (DEC), methyl ethyl carbonate (EMC) and dimethyl carbonate (DMC) aprotic solvent or ionic liquids (1-butyl-3-methylimidazolium bis(trifluoromethanesulfonyl)imide (BMITFSI) and 1-butyl-3-methylimidazolium tetrafluoroborate (BMIBF_4) 1-butyl-4-methylpyridinium bis(trifluoromethanesulfonyl)imide [BMPyTFSI]). Most of the polymer electrolytes have lithium hexafluorophosphate (LiPF_6) in ethylene carbonate (EC), dimethyl carbonate (DMC), propylene carbonate (PC), or diethyl carbonate (DEC) or their mixtures of various compositions. Polyvinylidene fluoride (PVdF) [3–7] and its copolymer polyvinylidene difluoride-*co*-hexafluoro propylene) (PVdF-*co*-HFP) [7–17], polyethylene glycol [18], polyurethane acrylate [19], polyacrylonitrile (PAN) [20–23], polymethyl methacrylate (PMMA) [22, 24, 25] and polyethylene oxide (PEO) [7, 17, 22, 26] polyvinyl acetate (PVAc) [25], polystyrene (PS) [22], etc., have been widely used as polymer matrices for the preparation of PEs. For improving the ionic conductivity, mechanical strength, and thermal stability, polymer nanocomposite electrolyte incorporating different ceramic nanomaterials

such as SiO₂ [27], Al₂O₃, [28] BaTiO₃ [11], TiO₂ [29, 30], ZrO [31], nanoclay [3, 9], etc., are also reported. The selection of materials and their proportions significantly influences the ionic conductivity, thermal stability and electrochemical properties of the polymer gel electrolytes [7].

In order to achieve high ionic conductivity at ambient temperature, many investigations have been reported. In recent years, much effort has been devoted to enhancing the low-temperature conductivity of PEs via various approaches such as the preparation of blends [32–34], copolymers [35–37], nanocomposites [38–40] and cross-linked networks [41, 42]. Improvements in ionic conductivity and electrochemical properties have been achieved either by reducing the crystallinity of the polymers or by lowering their T_g . Polymer blending and polymer nanocomposite preparation are found to be the most feasible among the techniques [43]. In the polymer blend electrolytes, polymers having complementary properties are used, such as one polymer have good electrochemical properties, and the other must be with good mechanical properties. The ionic conductivity and electrochemical/physical properties of polymer blend electrolytes are superior to that of the individual constituent polymers. In the blending, two or more different polymers are blend together to form a uniform mixture. Hence, the advantageous physical and electrochemical properties of different polymers can be making use in development of polymer gel electrolyte having improved properties. For example, PAN is blended with PMMA, the resulting polymer blend electrolytes of the CN groups in PAN could interact with CO groups of the liquid electrolytes such as propylene carbonate (PC), ethylene carbonate (EC), etc. as well with lithium ions [41], while the amorphous structure of PMMA is beneficial to ionic conduction and chemical cross-linking of the PMMA matrix can remarkably increase the mechanical strength and retention ability of the electrolyte solution [44]. In other words, the right materials choice to produce the gel electrolyte or battery separator for LIB is essential to achieve the appropriate and desired electrolyte characteristics [45]. The performance of a separator in a lithium-ion battery is determined by some requirements such as porosity, chemical and thermal stability, electrical insulator, wettability, dimensional stability, and resistance to degradation by chemical reagents and electrolytes [30, 46–48].

The membrane properties such as porosity, tortuosity and uniformity of pore distribution are strongly dependent on its processing method. Different methods such as solvent casting [49], plasticizer extraction [50], phase inversion [51] and electrospinning [52] have been reported for the membrane preparation. Compared to cast membranes, it is reported that the GPE based on electrospun membranes shows higher porosity, electrolyte uptake and ionic conductivity due to the presence of fully interconnected pore structure [51]. Electrospinning is a simple and versatile method which is gaining importance in recent years as membranes prepared by employing this method have controlled properties. The electrospun polymer membranes consist of thin fibers of micron/submicron diameters with high specific surface area. The interlaying of fibers generates large porosity (> 80%) with fully interconnected pore structure that can function as efficient channels for ion conduction thereby facilitates easy transport of Li⁺-ions and serves as good host matrices for GPEs [22]. Earlier

electrochemical studies of PEs based on electrospun membranes of PVdF [53], PVdF-*co*-HFP [51, 52], PAN [54] and PVdF-*co*-HFP/PAN blend [23] have demonstrated their potential application in lithium-ion batteries.

This chapter explains how the polymer gel electrolytes composed of two or more polymers are advantageously utilizing the beneficial electrochemical and physical properties for the individual polymers enhance the battery performance of LIBs [55–57]. The chapter covers two types of methods of preparation: (i) blending of polymers (binary blends and ternary blends) and (iii) layer-by-layer assembly of the thin layers of different polymers (trilayer assembly).

Electrospinning is one such technique which has received great attention due to its versatility in spinning of ultrafine fibers with a wide range of polymeric fibers also due to its consistency with uniform morphology in producing fibers ranging from micrometers to nanorange with porous structure [58]. Electrolyte membrane prepared by electrospinning has been reported in many literatures [59]. These membranes have large porosity with large surface area and interconnected network structure and uniform morphology. Electrospun blend electrolytes have the advantages of greater porosity with uniformity which enables easy pathways for ionic conduction, with these advantages, electrospun membranes as a host matrix for electrolyte.

8.2 Polymer Blend Electrolytes

8.2.1 PVdF or PVdF-*co*-HFP-Based Blend Electrolytes

Polyvinylidene difluoride or polyvinylidene difluoride (PVdF) is a highly nonreactive thermoplastic fluoropolymer produced by the polymerization of vinylidene difluoride, having the chemical formula $-(C_2H_2F_2)_n-$. PVdF is a specialty plastic used in applications requiring the highest purity, as well as resistance to solvents, acids and hydrocarbons. Currently, PVdF resins are widely used in LIBs as a binder material, both in anode and cathodes. PVdF is electrochemically stable in contact with electrolyte mixtures and has good affinity to liquid electrolyte. Also PVdF requires NMP (*N*-methyl 2-pyrrolidone) as a solvent and offers the possibility of high-voltage operation. PVdF is also electrochemically stable in contact with electrolyte mixtures. Hence, it is well-studied polymer matrix for the preparation of polymer electrolyte, and Sony is commercialized. PVdF and its copolymers (polyvinylidene difluoride-*co*-trifluoroethylene), polyvinylidene difluoride-*co*-trifluoroethylene (PVdF-*co*-TrFE), polyvinylidene difluoride-*co*-hexafluoropropylene (PVdF-*co*-HFP) and polyvinylidene fluoride-*co*-chlorotrifluoroethylene (PVdF-*co*-CTFE) show exceptional properties and characteristics for the development of battery separators, highlighting high polarity, excellent thermal and mechanical properties, wettability by organic solvents, being chemically inert and stable in the cathodic environment, and possessing tailorable porosity through binary and ternary solvent/non-solvent systems [60, 61]. Both the PVdF and its copolymers are partially fluorinated semi-crystalline polymers

Table 8.2 Major properties of these PVdF-based polymers

Polymer	Melting temp. (°C)	Degree of crystallinity (%)	Young's modulus (MPa)	Dielectric constant
PVdF	~170	40–60	1500–3000	6–12
PVdF-co-TrFE	~120	20–30	1600–2200	18
PVdF-co-HFP	130–140	15–35	500–1000	11
PVdF-co-CTFE	~165	15–25	155–200	13

where the amorphous phase is located between the crystalline lamellae arranged in spherulites. It can crystallize in different crystalline phase, depending on the temperature and processing conditions [62, 63]. In relation to the crystalline phases of PVdF and its copolymers, the most important phases are the β -phase, since it presents ferroelectric, piezoelectric, and pyroelectric properties, and the α -phase, which is the most stable thermodynamically, when material is obtained directly from the melt [62]. PVdF has a strong electron withdrawing fluorine atom in its back bone and high dielectric constant ($\epsilon = 8.4$). Thus, the polymer blend effectively dissociates lithium salts to generate a large quantity of charge carriers for conduction [64, 65]. The major physical and electrical properties of these PVdF-based polymers are presented in Table 8.2 [55, 66–68].

8.2.1.1 Blend with PMMA

Polymethyl methacrylate (PMMA), a synthetic resin produced from the polymerization of methyl methacrylate having the chemical formula $-(C_5O_2H_8)-$. PMMA is a transparent and rigid thermoplastic material often used as a substitute for glass in products such as lightweight or shatterproof windows, skylights, illuminated signs and aircraft canopies. PMMA is an economical alternative to polycarbonate (PC) when tensile strength, flexural strength, transparency, polishability and UV tolerance are more important than impact strength, chemical resistance and heat resistance. PMMA is one of the host polymers previously used in plasticized PEs, which was first reported by Iijima et al. and more recently by Bohnke et al. [69] and others Zhang et al. [22, 25] Appetecchi et al. [70] studied the kinetics and stability of the lithium electrode in PMMA-based gel electrolytes. PMMA is a common thermoplastic polymer with well-known chemistry. Its amorphous structure is beneficial to ionic conduction and PMMA-based gel electrolytes have shown excellent interfacial stability toward lithium metal. The pendant $-COOCH_3$ is not likely to crystallize around Li^+ as PEO does. PMMA-based PEs exhibit high electrolyte uptake, ionic conductivity and good electrochemical stability [71]. Unlike PAN, PMMA has ability to make chemical cross-linking, which will remarkably increase the mechanical strength and the electrolyte solution retention ability of the PE [72, 73]. Also it has been reported that gel electrolytes based on cross-linked PMMA can suppress lithium dendrite formation [72]. However, they suffer from a gel-like mechanical

property: They do not form a free-standing film at high plasticizer content or the electrospun PMMA fibers are very brittle. Thus, an improvement in the mechanical properties of PMMA-based PEs is required to make them suitable for commercial applications. A blend of PMMA with PVdF [74, 75] and PVdF-*co*-HFP [76]-based electrospun polymer gel electrolytes are prepared by activating the fibrous membrane with 1 M LiClO₄ in PC (propylene carbonate) [74] or 1 M LiPF₆ (lithium hexafluorophosphate) in EC:DMC (1:1 v/v) (ethylene carbonate and dimethyl carbonate) solution [75, 76] were reported.

A blend of PVdF-PMMA (80:20 wt./wt.) electrospun fiber showed the fiber diameter of 183 [75] and 325 nm [74]. The higher fiber diameter observed for the same PVdF-PMMA blend is due to the higher spinning voltage and higher feed rate. They showed an electrolyte uptake of 275 (1 M LiPF₆ in EC:DMC) [75] and 285% (1 M LiClO₄-PC) [74] even both the membranes have similar porosity of about 85%. The membrane activated with 1 M LiClO₄-PC is showed higher ionic conductivity ($2.95 \times 10^{-3} \text{ S cm}^{-1}$) at RT [74]. This difference in uptake may come from the difference in affinity of the membrane to the different electrolyte, thereby shows the difference in ionic conductivity. The average fiber diameter of PVdF and PVdF-PMMA (50:50) is found to be 647 and 179 nm (Fig. 8.3). PVdF-PMMA (50:50) polymer electrolyte membrane showed an electrolyte uptake 290% (porosity 87%) and ionic conductivity of 0.15 S cm^{-1} and at room temperature, while the pristine PVdF membrane showed lower porosity (78%), electrolyte uptake (260%) and ionic conductivity (0.1 S cm^{-1}) (Table 8.3). The Li/PE/LiFePO₄ cells with 1 M LiPF₆ in EC: DMC as electrolyte delivered an initial discharge capacity of 138.4, 144.7 and 150.3 mAh g⁻¹ for separators of PVdF, PVdF/PMMA (80:20) and PVdF/PMMA (50:50) membranes, respectively. After 50 cycles, the cell with PVdF-PMMA (50:50) electrolyte retained a discharge capacity of 140 mAh g⁻¹ which is about around 93% retention of the initial discharge capacity, while the pristine PVdF membrane retained a discharge capacity of only 130 mAh g⁻¹ (~94% retention). Nanofibrous PVdF-PMMA (50:50) polymer electrolyte membrane was found to be a potential separator for lithium-ion batteries. Compared with cells having different PEs, discharged capacity for the cell with PVdF-PMMA (50:50) separator was found to be relatively high cathode utilization corresponding to 88.4% of theoretical capacity which is 3.5% higher than that of PVdF-PMMA (80:20) polymer blend electrolyte [75].

The PVdF-*co*-HFP blend with PMMA could be expected to have higher ionic conductivity than that with PVdF, due to the lower crystallinity of PVdF-*co*-HFP result from the presence of HFP in the copolymer. The PMMA blend polymer electrolyte having ~66% PVdF-*co*-HFP shows an ionic conductivity of 2 mS cm^{-1} [76], while the blend having only 50% PVdF showed an ionic conductivity of only 0.15 S cm^{-1} [75].

The fiber diameter of pristine PVdF-*co*-HFP nanofibers was found to be 100–250 nm, and the surface of the fibers was very smooth due to its homogeneous polymeric texture. The fibers are randomly oriented, and most of the fibers were not interconnected. However, by blending with PMMA (about 33%), the average diameter of the fibers increased (200–350 nm) and the nanofibers were frequently

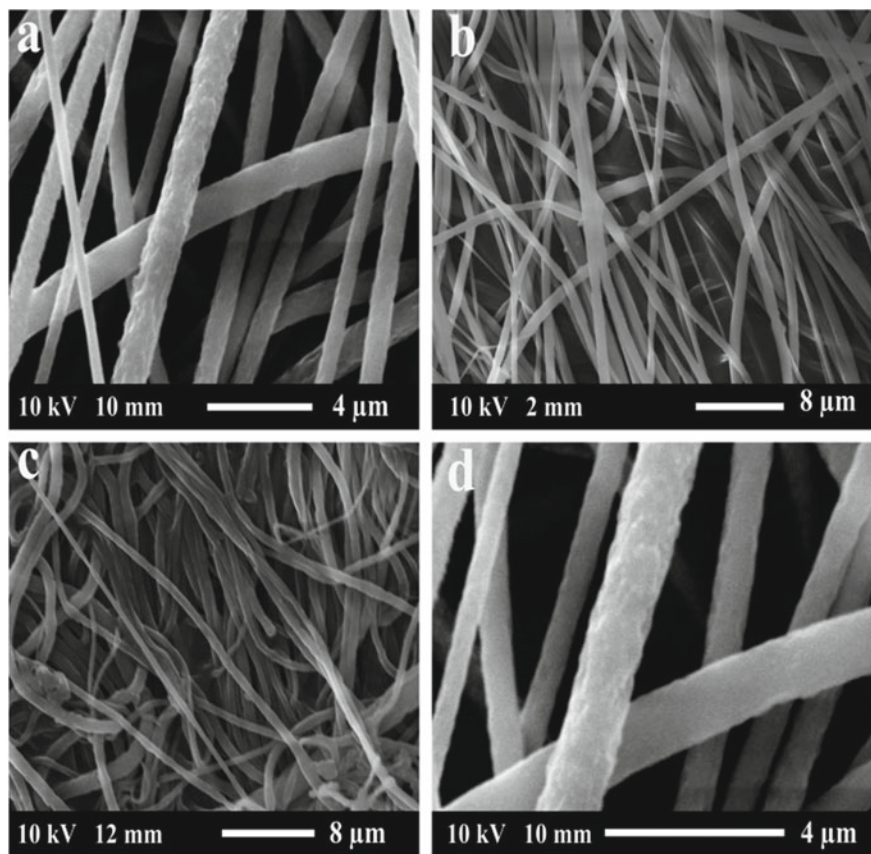


Fig. 8.3 SEM images on the surface morphology of electrospun polymer blend nanofibrous membranes of **a, d** pristine PVdF, **b** PVdF-PMMA (80:20), **c** PVdF-PMMA (50:50) Adapted and reproduced from Ref. [75]. Copyright 2018 Springer

Table 8.3 Melting enthalpy (ΔH_f), crystallinity (χ_c), bulk resistance (R_b) and ionic conductivity (σ) of PVdF, PVdF/PMMA (80:20) and PVdF/PMMA (50:50) nanofibrous membranes [75]

Polymer membranes	ΔH_f (J/g)	χ_c (%)	R_b (Ω)	σ (S/cm)
PVdF	53.29	50.75	0.50	0.10
PVdF:PMMA (80:20)	43.84	41.75	0.29	0.13
PVdF:PMMA (50:50)	25.33	24.12	0.22	0.15

interconnected by fusing the attaching point of two or three individual fibers. Furthermore, in comparison with the pristine PVdF-co-HFP nanofibers, the surface of the composite nanofibers became rough, which will be beneficial for getting better interfacial contact with electrode and lowering the interfacial resistance between the electrode and electrolyte. The PVdF-co-HFP/PMMA blend polymer membrane

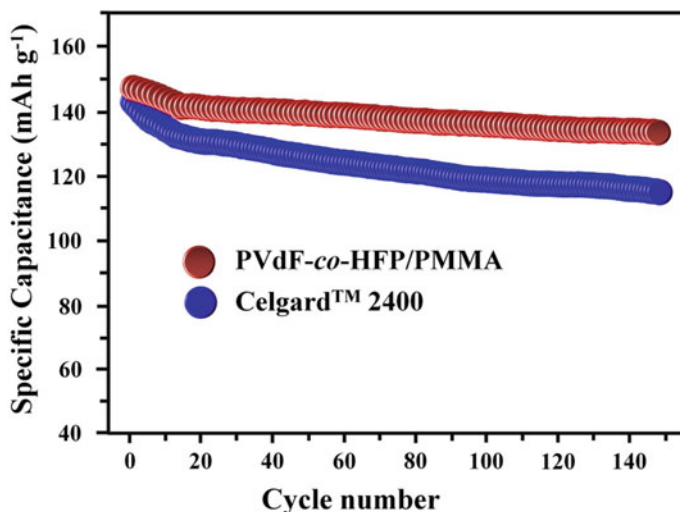


Fig. 8.4 Cycle performance of the prototype cells. Li/PE/LiFePO₄ prototype cells with cutoff voltages of 2.4 and 4.1 V at 0.1C-rate. Adapted and reproduced from Ref. [76]. Copyright 2009 Elsevier

showed an uptake and leakage for electrolyte solution of 377% and 87% which is about 75% and 11% higher than pristine PVdF-co-HFP membrane, respectively. The Li/PE/LiFePO₄ cell with PVdF-co-HFP/PMMA blend polymer electrolyte or commercial Celgard TM 2400[®] shows comparable initial discharge capacities ~145 mAh g⁻¹; however, the cells with electrospun PVdF-co-HFP/PMMA electrolyte showed a stable discharge behavior and little capacity loss under constant current conditions, which still retained a capacity of 133.5 mAh g⁻¹ (92% retention) after 150 cycles. However, the cell with Celgard TM 2400[®] showed a remarkable capacity fading and the capacity decreased to 115 mAh g⁻¹ (79% retention) after 150 cycles (Fig. 8.4). The improved cycle performance of the prototype cells with electrospun PVdF-co-HFP/PMMA could be ascribed to the lower leakage in the sandwich structure of the cell and higher porosity [76]. The crystallinity of both PVdF and PVdF-co-HFP has been depressed with increasing PMMA content, because the motion of PVdF or PVdF-co-HFP chains during the crystallization was hindered by the bulky CH₃OCO—group in PMMA chains. Moreover, the crystallinity has been depressed by the hydrogen bonds between the PMMA and PVdF or PVdF-co-HFP chains. Lowering the crystallinity leads to higher ionic conductivity [75, 76].

8.2.1.2 Blend with PEO

Polyethylene oxide (PEO) is also known as PEG was the first example of a single-chain single crystals having the chemical formula H-(O-CH₂-CH₂)_n-OH. C_{2n}H_{4n+2}O_{n+1} PEO-based polymer electrolytes have received extensive attention for

their potential usage as alternative materials for traditional organic liquid electrolytes (OLEs) since Fenton et al. [77] found that the complex of PEO with alkaline salts possesses good ionic conductivity. Followed by this report, (PEO)-based electrolyte has been widely studied as all solid polymer electrolytes in LIBs. PEO has low glass transition temperature (T_g), good chain flexibility, thermal properties, mechanical properties, superior electrochemical stability to lithium metal, and excellent solubility with conductive lithium salts are poised to be an enabler for solid-state lithium batteries, but their application is restricted by low room-temperature ionic conductivity and poor mechanical strength at elevated temperatures [78, 79]. It has ether linkages, with oxygen atoms present at a suitable inter-atomic separation to allow segmental motion of the polymeric chain which is beneficial for facile ionic conduction [80–82]. It is widely accepted that PEO can form complexes with a large number of lithium salts and transport Li^+ -ions in PEs. Thus, significant ion conduction occurs in the amorphous phase where the conductivity is two or three orders of magnitude higher than in the crystalline region [83]. The high crystallinity of PEO leads to low ion conductivity ($10^{-8} \times 10^{-6} \text{ S cm}^{-1}$) and inferior Li^+ transference numbers (0.2–0.3) at room temperature, which seriously affects the high rate capability of LIBs. This necessitates operation at higher temperatures (generally, $>70^\circ\text{C}$) for their successful utilization in practical battery applications. The Li^+ -ion transport in these all solid-state polymer electrolytes has been associated with the local relaxation and segmental motion of the amorphous regions in the PEO chains. Ethylene oxide (EO) segment in the PEO is soluble in common battery electrolytes like ethylene carbonate (EC) and diethyl carbonate (DEC), which limits its use in dimensionally stable PGEs, therefore, blending of PEO with other polymers are the widely adopted method the preparation of PEO-based polymer gel electrolytes [83, 84]. Prasanth et al. reported electrospun-based polymer gel electrolyte prepared by blending of PEO with PVdF [7] and the polymer blend incorporated with ceramic filler [17]. The aim of the study was to develop polymer gel electrolyte (PGE) which utilizes the advantageous electrochemical properties of PEO to make them for the practical application in LIBs and study the effect of PEO on ionic conductivity and electrochemical properties of PVdF-based PGEs. The presence of PVdF in the polymer blend retains the mechanical properties of the membrane, while the ether linkages with oxygen atoms in PEO help to improve the segmental motion and dissociation of lithium salts. The surface morphology of PVdF/PEO blend membranes is displayed in Fig. 8.5.

The PVdF/PEO blend (5–20 wt% PEO content) electrospun membranes with [17] and without [7] nanosized ceramic filler (LAGP) were prepared first. Then, the blend polymer membrane incorporated with nanosized LAGP is immersed in the boiling water for the preferential isolated and removed removal of PEO from the blend fiber [17]. The surface morphology of electrospun membrane before and after in situ porosity generation (Fig. 8.6) and the Fig. 8.7 shows the surface morphology of the PVdF/PEO blend membranes before and after soaking in the hot water. The immersing of membrane in hot water (70°C) for 48 h, the PEO partially leach out from the micron-sized fibers. PEO is water soluble, while PVdF is not; therefore, PEO was preferentially isolated and removed from the membranes, leaves nanopores

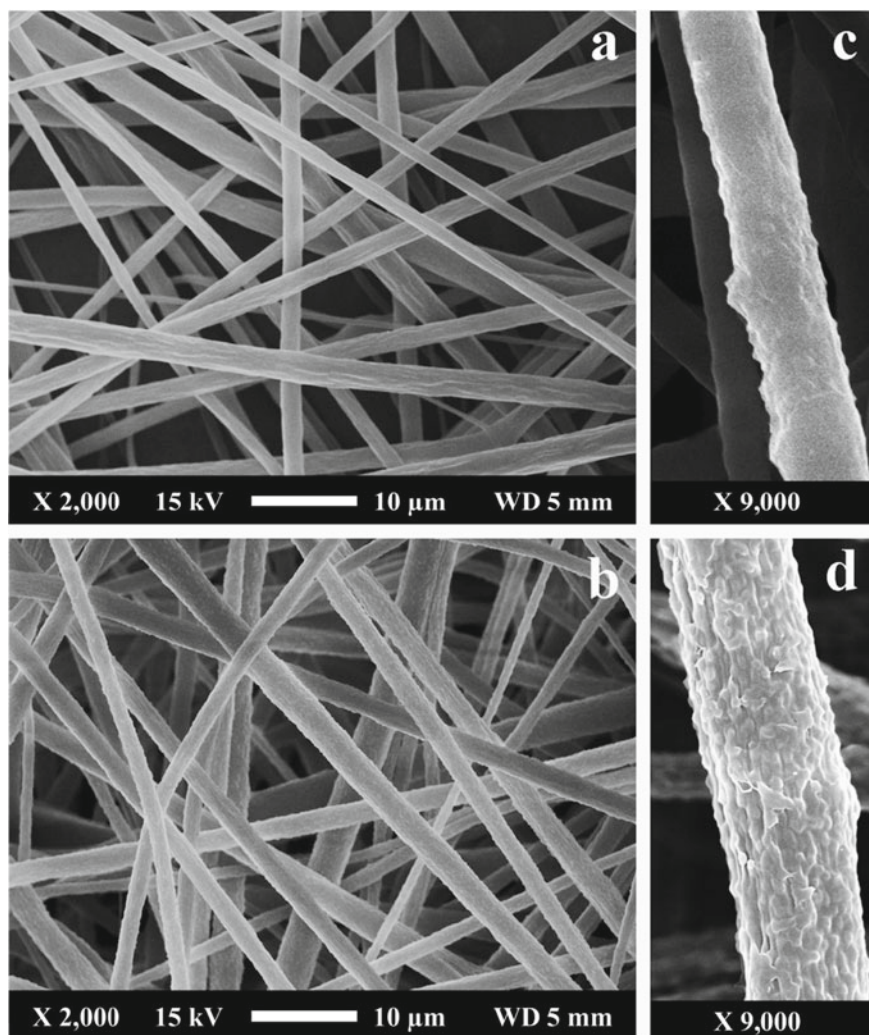


Fig. 8.5 FE-SEM images on the surface morphology of electrospun membrane; **a** pristine PVdF, **b** PVdF/PEO (90:10) blend; magnified image of fiber; **c** pristine PVdF, **d** PVdF/PEO (90:10) polymer blend fiber. Adapted and reproduced from Ref. [7]. Copyright 2014 Elsevier

uniformly distributed on the surface of the nanofibers. The pore density was directly related to the PEO content in the polymer blend. Porosity is one of the key factors which determine the ionic conductivity and electrochemical performance of polymer electrolytes based on electrospun membranes in lithium-ion batteries [9]. Higher porosity can enlarge the contact area between the polymer and liquid electrolyte, which ensures that the electrolyte well retained in the polymer membrane leads to

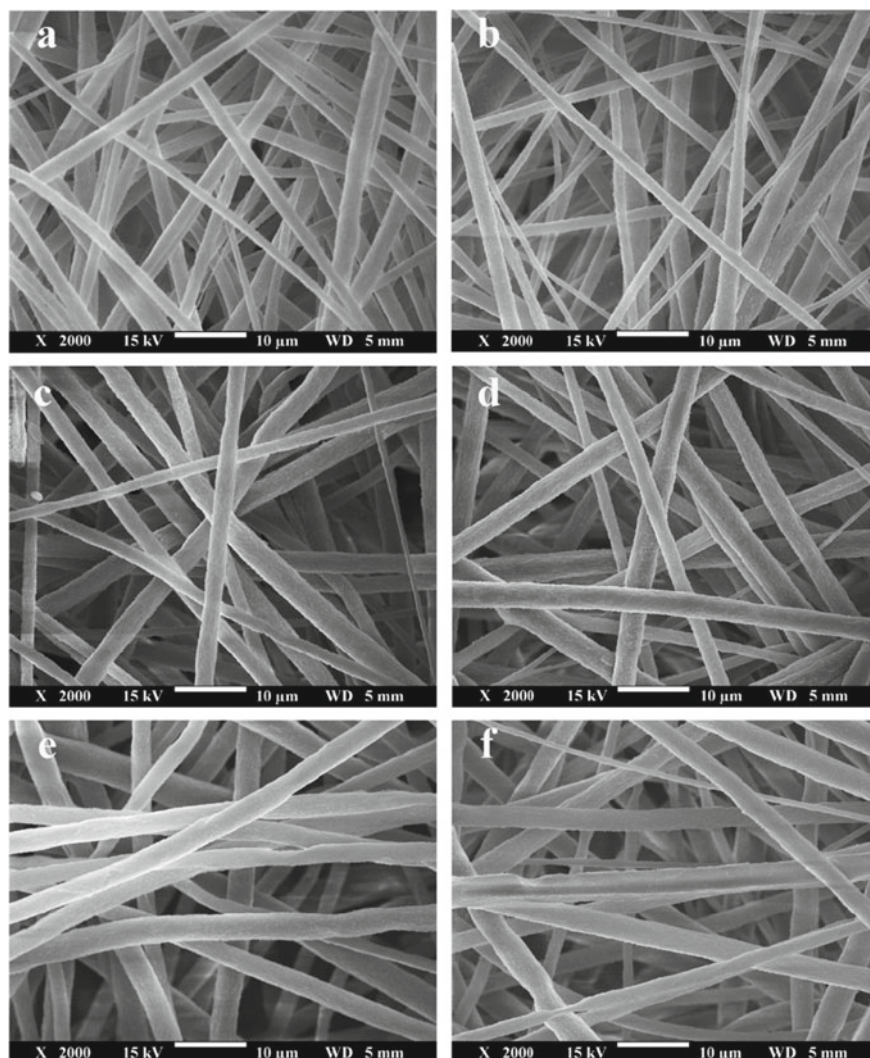


Fig. 8.6 Surface morphology of electrospun PVdF/PEO polymer blend with membranes with lithium aluminum germanium phosphate (LAGP) glass ceramic lithium ion conducting filler (PVdF:LAGP, 94:6 wt%) having x wt% PEO on the total weight of PVdF and LAGP: before **a** ESM-01 ($x=5$), **c** ESM-02 ($x=10$), **e** ESM-03 ($x=20$) and after **b** IPG-01 ($x=5$), **d** IPG-02 ($x=10$) and **f** IPG-03 ($x=20$) soaking in hot water. (ESM-as spun membrane, IPG-in-situ porosity generated membrane). Adapted and reproduced from [17]. Copyright 2014 Elsevier

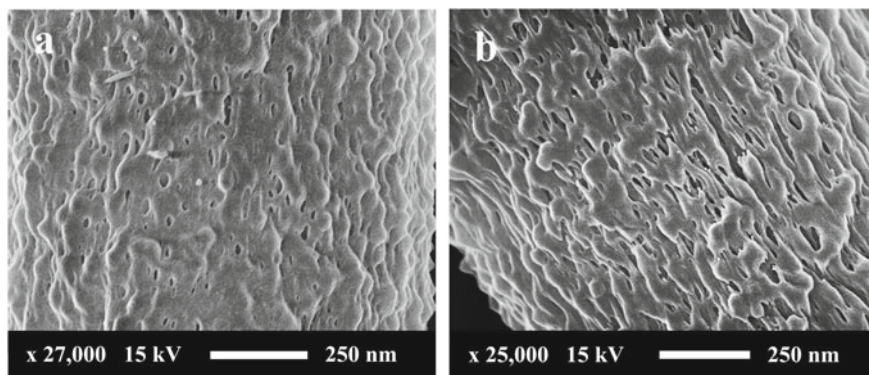


Fig. 8.7 Magnified images of surface morphology of electrospun PVdF/PEO polymer blend fibers with lithium aluminum germanium phosphate (LAGP) glass ceramic lithium ion conducting filler (PVdF:LAGP, 94:6 wt%) having x wt% PEO on the total weight of PVdF and LAGP; **a** IPG-02 ($x = 10$) and **b** IPG-03 ($x = 20$). (IPG-in-situ porosity generated membrane). Adapted and reproduced from [17]. Copyright 2014 Elsevier

the long term cycling stability of LIBs. The effect of PEO on the pore formation and electrochemical properties of the blend electrolyte is shown in Table 8.4.

The blend polymer electrolytes showed higher charge–discharge and cycling stability compared to pristine PVdF electrolyte or commercial Celgard® separator. The lithium cell assembled with Li metal/LiFePO₄ electrode and PVdF/PEO blend (10% PEO) PGE based on LiTFSI or LiClO₄ delivers an initial discharge capacity of 165–168 mAh g⁻¹, which corresponds to w 98 ± 1% utilization of the active material. While the cell with PGE based on electrospun PVdF showed a discharge capacity of 148 mAh g⁻¹, which is about 11% less than the cell with PGE based on PVdF/PEO polymer blend membrane at a current density of 0.1C. After 50 cycles, the cell comprised of PVdF membrane activated with LiTFSI and LiClO₄ delivers a discharge capacity of ~128 mAh g⁻¹. The capacity retention ratio of the cell with PVdF/PEO polymer blend membrane activated with LiTFSI electrolyte is 95%, and LiClO₄ is 89% (calculated based on initial discharge capacity), while the cell with PVdF membrane shows only w 86% retention. [7]. However, the PVdF/PEO blend electrolyte, from which PEO is leached out, showed lower initial specific capacity compared to the one without leaching process. The initial capacity was found to be about 130 to 150 mAh g⁻¹ with LiTFSI, where the membrane prepared with higher PEO content delivered higher capacity. After 50 cycles, the cells delivered a discharge capacity of 126, 137 and 150 mAh g⁻¹ respectively, for the PVdF/PEO blend electrolyte prepared with 5, 10 and 20 wt% PEO and soaked in hot water for the preferential leaching. The rate capability studies reported that at low C-rates (0.1–0.6 C), both the cell with conventional Celgard® or PVdF/PEO blend electrolyte membranes delivered similar capacities, but at higher C-rates (1.5–3.0 C), the blend electrolyte membrane shows considerably higher capacity compared to the conventional Celgard® and retain similar capacity after the current density is changed back

Table 8.4 Properties of polymer electrolyte membranes activated with different lithium salt in electrolytes (electrolyte: 1 M solution of lithium salt in 1:1 w/w EC/DEC)

Membrane	Lithium salt in EC/DEC	Porosity (%)	Electrolyte uptake (%)	Crystallinity (%)	Ionic conductivity at 30 °C (mS cm ⁻¹)
PVdF/PEO (90:10)	LiTFSI	85	750	42.3	4.9
PVdF/PEO (90:10)	LiPF ₆	85	690	42.3	4.5
PVdF/PEO (90:10)	LiClO ₄	85	675	42.3	4.2
PVdF/PEO (90:10)	LiBF ₄	85	630	42.3	2.8
PVdF/PEO (90:10)	LiCF ₃ SO ₃	85	590	42.3	1.8
PVdF/PEO (95:05) + 6 wt% LAGP	LiTFSI	78	632	39.1	6.3
PVdF/PEO (90:10) + 6 wt% LAGP	LiTFSI	80	652	40.4	7.0
PVdF/PEO (80:20) + 6 wt% LAGP	LiTFSI	83	703	42.6	7.7
PVdF/PEO (95:05) + 6 wt% LAGP (after leaching)	LiTFSI	85	723	36.8	8.0
PVdF/PEO (90:10) + 6 wt% LAGP (after leaching)	LiTFSI	89	768	38.2	9.1
PVdF/PEO (80:20) + 6 wt% LAGP (after leaching)	LiTFSI	93	831	38.8	10.9
					at 35 °C
PVdF	LiPF ₆	80	650	40.5	3.2
PVdF/PEO	LiPF ₆	85	690	42.3	5.3
Celgard (2320)	LiPF ₆	41	200		2.1 × 10 ⁻²

to 0.2 C-rate after 40 cycles, which clearly demonstrates high capacity retention of the cells [17]. Again by blending PVdF with PEO, the LSV of the blend electrolyte is >5 V, which is considerably higher than PVdF-co-HFP-based electrospun polymer gel electrolytes (4.5 V) [13, 14, 51] Also the interfacial resistance with Li/Li metal was found to be 10–22 Ω [7, 17], which is much lower than that of 750–800 Ω for PVdF-co-HFP-based electrospun polymer gel electrolytes [11, 14].

8.2.1.3 Blend with Polydiphenylamine (PDPA)

Polydiphenylamine (PDPA), a polymer of *N*-substituted aniline preparing by oxidative polymerization [85, 86]. It is more soluble in common organic solvents and exhibits different redox characteristics than other poly(*N*-substituted anilines) [87, 88]. The backbone units of PDPA can be grafted with other polymeric chains to have novel functional properties [89] To utilize these unique properties, Gopalan et al. [90] blended PDPA with PVdF or its copolymer PVdF-co-HFP for the preparation of polymer gel electrolyte. Electrospun membranes blended PDPA/PVdF or PDPA/PVdF-co-HFP having different thickness ranging from 20 to 60 μm were prepared by electrospinning. The PDPA content in the blend was 0.5–2 wt%. The electrospun membranes were transformed to pole electrolyte by activating with 1 M LiClO_4 -PC solution. The electrospun polymer blend membrane exhibited morphological variations with PDPA content Fig. 8.8. Electrospun pristine PVdF fibrous membranes have a nearly straightened and tubular structure with an average fiber diameter of ~ 500 nm. The PDPA/PVdF has interconnected multifibrous layers with ultrafine porous structures. The presence of PDPA significantly affected average fiber diameter. The average fiber diameter decreased with increasing PDPA content and the fibers appeared to be uniform in composition without having any phase separated microstructure or beads morphology reveals the miscibility and compatibility of PVdF and PDPA. By blending PVdF with 0.5 wt% PDPA, the average fiber diameter is down to 200 nm. There is inter-fiber twisting in the PVdF/PDPA

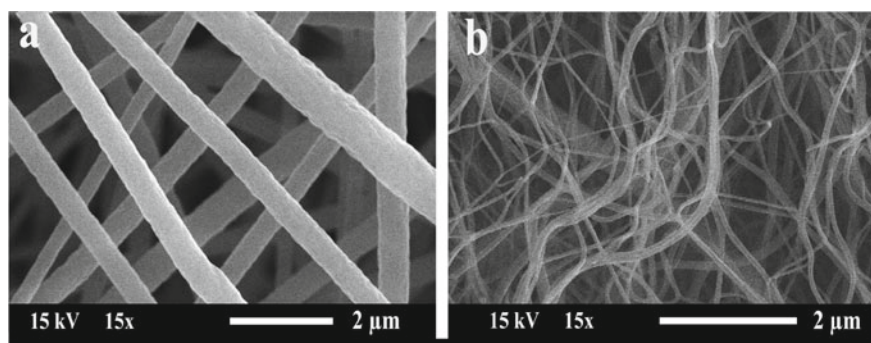


Fig. 8.8 FE-SEM images on the surface morphology of electrospun **a** PVdF, **b** PVdF-PDPA-CFM with PDPA (wt%) **a.** 0.5 and **b.** 1. Adapted and reproduced from Ref. [90]. Copyright 2008 Elsevier

that generates microcavities and entanglements between the fibers are more with higher PDPA content. The difference morphology and fiber diameter between the pristine and PDPA/PVdF blend membranes can be possible due to the difference in the spinning parameters (distance between the nozzle and the collector, applied voltage and feed rate); however, all these parameters are kept constant in the study. Hence, the following factors may be influenced on the morphological difference in the membranes [90];

- (i) Difference in viscosity of the spinning solutions (the incorporation of PDPA can increase the viscosity of the polymer solution due to the presence of aromatic ring in the polymer)
- (ii) Difference in dielectric constant of the spinning solutions (the incorporation of PDPA can increase the dielectric of the medium for electrospinning)

Because of higher dielectric solution (in comparison to a lesser dielectric pristine PVdF solution) could easy to form a Taylor cone at the tip of the spinning needle of the syringe which result in the formation of smooth thin fibers without any beads [15]. The formation of interconnected and entangled fibrous morphology of the PDPA/PVdF blend membrane could be arise from the probable intermolecular interactions between the protonated amine or imine groups in PDPA [7, 8] and electronegative fluorine atoms in PVdF.

The electrolyte uptake, ionic conductivity, lithium transference number, anodic stability (>5 V) and interfacial properties are increased with PDPA content. PVdF/PDPA with 2 wt% PDPA showed an electrolyte uptake >280 wt% which is 80% higher than pristine PVdF membrane. The uptake value is considerably higher than reported values for PVdF, [20–24] but significantly less compared to the uptake for PVDF or PVdF-*co*-HFP membranes reported by Prasanth et al. [11, 14]. The polymer blend electrolyte with 2% PDPA (60- μ m thickness) exhibits an ionic conductivity of 3.6 mS cm^{-1} at 25°C , which is higher than reported value for PVdF-based electrolyte [91–95] and the lithium transference number (t_+ value) of 0.48. The reported t_+ values for SPEs range from 0.06 to 0.2 [96]. For gel polymer systems, t_+ values in the order of 0.4–0.5 have been reported. Cationic transport number ranging between 0.2 and 0.4 has been reported for PVdF-*co*-HFP-based electrolyte membrane [97–100].

The higher ionic conductivity for PVdF/PDPA fibrous electrolyte is attributed to arise from the combined influence of higher content of electrolyte (>280 wt%) incorporated into the pores of the membrane and augmented lithium-ion mobility in the membrane. Doped PDPA has positively charged nitrogen sites (protonated diphenylquinone diamine units) [87, 88]. That have molecular-level interactions with the electronegative fluorine atoms present in PVdF. This environment provides (i) new path for Li^+ -ion migration in the composite, (ii) interconnected network morphology between PDPA and PVdF and (iii) compact porous structure to hold more amount of the liquid electrolyte. The recombination possibility of Li^+ -ion with ClO_4^- ion is expected to be hindered in the presence of PDPA, and hence, facile Li^+ -ion mobility becomes possible. A portion of the ClO_4^- ions is expected to be immobilized at the

protonated amine or imine sites of PDPA by replacing the organic dopant, naphthalene sulfonate anions. The bulky naphthalene sulfonate anion has lesser mobility than ClO_4^- ion. As a result, Li^+ -ions in the PVdF/PDPA membrane matrix can freely move to result higher ionic conductivity. In the pouch cell, the charge–discharge studies of PVdF blend electrolyte with 1 and 2 wt% PDPA content, in the full cell configuration using graphite anode and LiCoO_2 cathode under different C-rate shows similar discharge capacity in lower C-rate (0.2–0.5 C), but at the higher C-rate (at a C-rate higher than 0.5 C) the cell with blend electrolyte having higher PDPA content delivers higher discharge capacity which is due to the high ionic conductivity and highly porous morphology of PVdF/PDPA electrospun membrane. Typically, at 1 C-rate, the cell can deliver about 90% of its 0.2 C capacity, and even the C-rate is doubled (at a high rate of 2 C), and the cell can still deliver about ~70% of its 0.2 C capacity. Also, the cell delivered about 95% of its initial capacity after 50 continuous charge–discharge cycles at 1 C (25 °C).

8.2.1.4 Blend with Polyvinyl Chloride (PVC)

Polyvinyl chloride having the chemical formula $(\text{C}_2\text{H}_3\text{Cl})_n$ is the world's third-most widely produced synthetic plastic, after polyethylene and polypropylene, which is used for the preparation of commercial battery separator Celgard®. About 40 million tones are produced per year. The presence of chlorine in the polymer backbone of PVC makes them as a self-extinguishing polymer. PVC is an inexpensive material has low dielectric constant ($\epsilon \approx 3$), good processability, which can act as good mechanical stiffener. In the recent years, PVC-based PEs gained much popularity due to their good compatibility with many polymers and easiness to prepare a hard brittle plastic to a rubbery material by simply plasticizing with suitable plasticizer [71, 101, 102]. Many literatures [103–105] showed that PVdF and PVC can be blended as the PEs. The addition of PVC was used to suppress the crystallinity, thereby enhancing the ionic conductivity, to reduce the thermal stability [102] due to the decomposition of PVC in the membrane. The decomposition temperature of PVC is about 285 °C which is significantly lower than that of PVdF (~450 °C) [102].

PVC-based gel polymer electrolyte, blend with PVdF, PAN, poly (butyl methacrylate) [PBMA], PEMA, ionic liquids, etc., are reported either cast films or electrospun-based membranes. The PEs based on PVdF/PVC prepared by casting technology have been earlier reported by Rajendran et al. [103] and Muniyandi et al. [105]. Their results demonstrated that the PEs prepared by casting technology had a low ionic conductivity and poor cycling behavior. Thus, nanofibrous membranes based on PVdF/PVC (8:2, w/w) were prepared by electrospinning and then activated with 1 M LiClO_4 in PC/EC (1:1 v/v) to transform polymer gel electrolytes. The electrolyte uptake and ionic conductivity studies revealed that the blending of PVdF with PVC is beneficial to enhance the polymer gel electrolyte characteristics. Both the electrolyte uptake and ionic conductivity of the blend electrolyte increase with the PVC content. The higher ionic conductivity of the blend electrolyte is directly related to the higher electrolyte uptake and lowering of crystallinity by the PVC

phase in the blend polymer gel electrolyte. By blending the PVdF with 20 wt% of PVC reduces about 22% crystallinity of PVdF (38.4%), which leads to the formation of more gelled phase in the blend polymer electrolyte. The lower fiber diameter also enhances the gelled phase in the electrolyte. Even though both the membranes identical morphology having fully interconnected porous structure composed of ultrafine straight fibers, the average fiber diameter (AFD) and fiber diameter distribution are significantly different (Fig. 8.9). The diameters of PVdF nanofibers are ranging from 257 to 1380 nm (AFD is 932 nm) (Fig. 8.9a) for the pristine PVdF membrane, while that is in the range of 385–875 nm (AFD is 624 nm) (Fig. 8.9b) for the PVdF/PVC blend membrane [106]. The considerably lower average fiber diameter could offer higher surface area which beneficial for the absorption of large quantity of liquid electrolyte and the formation of more gelled phase in the polymer electrolyte. The lower ionic conductivity of pristine PVdF-based electrospun gel electrolyte compared to PVdF/PVC blend counterpart can be attributed to the slower conduction path in the swollen polymer phase in the nanofiber due to the higher crystallinity. Hence, the

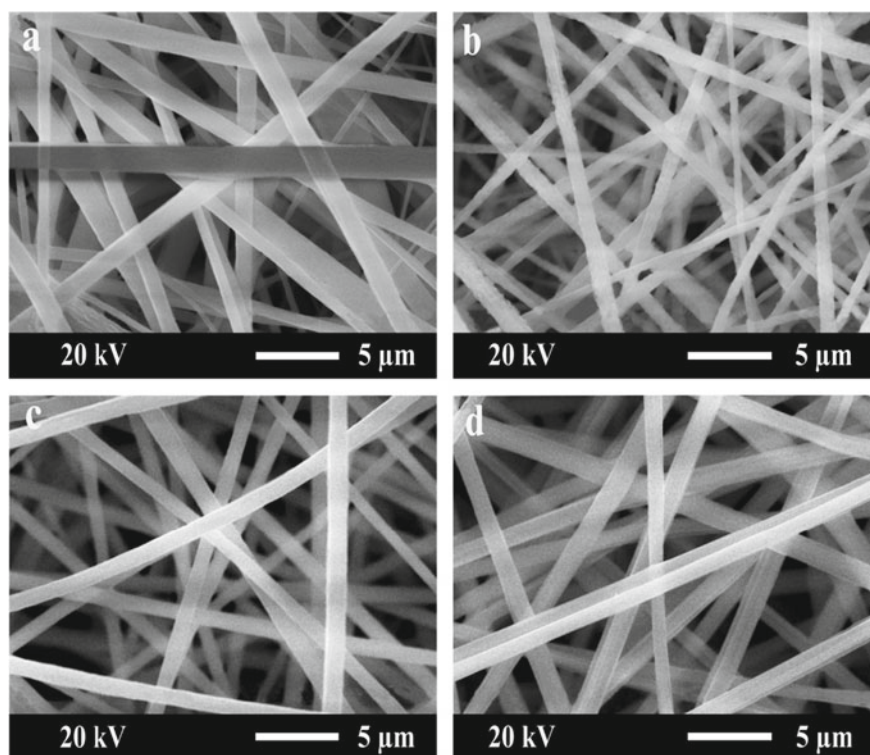


Fig. 8.9 SEM photographs on the surface morphology of **a** pristine PVdF, **b** PVdF-PVC (8:2) membrane, Adapted and reproduced from Ref. [107], Copyright 2012 Elsevier PAN-PVC polymer membrane, **c** pristine PAN, **d** PAN: PVC (8:2), Adapted and reproduced from Ref. [106], Copyright 2012 Springer

lower crystallinity of the blend polymer electrolyte promotes the mobility of the Li^+ -ion, thereby lowering the activation energy for the Li^+ -ion transportation in the electrolyte [21]. The PVdF/PVC polymer blend gel electrolyte displayed high ionic conductivity up to 2.25 mS cm^{-1} , which is about 35% higher than that of while pristine PVdF membranes at 25°C . The ionic conductivity of pristine PVdF and PVC electrospun gel electrolyte was found to be 1.47 and 0.66 mS cm^{-1} at 25°C . The Li/PE/LiFePO₄ charge–discharge studies showed about 85.4% cathode unitization (145 mAh g^{-1}) in the first cycle at a current density of 0.1 C with a Columbic efficiency of (ratio between charge and discharge capacity) is 98.6%. After 50 cycles, the discharge capacity of the cell retained a discharge capacity of 130.8 mAh g^{-1} which is still 90.1% of the initial discharge capacity, which is an indication of good cycling stability and good interfacial stability between the electrode and the PVdF/PVC blend polymer membranes [90]. These results suggest that the nanofibrous polymer gel electrolytes based on PVdF/PVC have great potential in polymer lithium-ion batteries [107]. Blending of PAN with PVC results the three-dimensional network structure (Fig. 8.9c, d) that able to absorb large amounts of liquid electrolyte. The average fiber diameter (AFD) of the electrospun fibrous membranes is 890, 1,100, respectively, that contains PAN and PVC in the ratio 10:0 and 8:2. This variation in AFD is attributed by the difference in viscosity of the polymer solution and its rheological properties. Even though the ionic conductivity of this blend is lower than that of pure PAN, the mechanical strength is observed to be increased, that make it for the practical use. However, the blend film with PAN: PVC (8:2) exhibits an ionic conductivity of $1.05 \times 10^{-3} \text{ S cm}^{-1}$ which is apt to use in lithium-ion batteries [106].

8.2.1.5 Blend with Polypropylene Carbonate (PPC)

Polypropylene carbonate (PPC) having a chemical formula $[\text{CH}_2(\text{CH}_2\text{CO}_2)_n$ has recently received considerable attention. Since this unique polymer is synthesizing by copolymerizing carbon dioxide (CO_2) and propylene oxide (PO), it can effectively reduce CO_2 emissions and mitigate the greenhouse effect [108–112]. Aside from this, it is a completely biodegradable and a good substrate material for the preparation of environmentally friendly polymer electrolytes [111, 112]. PPC-based gel electrolytes are widely tested in LIBs. PPC has similar structure to carbonate-based solvents, which is commonly applied in conventional gel electrolytes as a plasticizer, and carbonate solvent for dissolving the lithium salt [35] suggests that it could offer good compatibility as well as interfacial contact with commonly using battery electrodes. In addition, the polar ester group in the polymer backbone can effectively trap and store liquid electrolyte, thereby showing high electrolyte absorption, ionic conductivity and lithium transference number. The higher lithium transference number results from the presence of amorphous aliphatic polycarbonate with low glass transition temperature (T_g) that leads to the local relaxation and segmental motion of PPC chain, which is favorable for the Li^+ -ions transportation at lower activation energy. In addition, the polar ester groups facilitate PPC chains to a solvent gelator owing to their strong interactions with the common organic liquid

electrolyte. Even though PPC shows high electrolyte uptake, the low mechanical properties and poor thermal stability of pristine PPC-based polymer gel electrolytes restrict its successful application in LIBs. To overcome this problem and make their practical use in LIBs, the most straightforward approach is to modify the PPC to achieve enough mechanical strength and thermal stability while retaining a high volume fraction of the conductive amorphous phase and the outstanding electrolyte uptake. Among different methods such as structural modification [30], incorporation of reinforcing nanoceramic fillers [11], blending with mechanically strong and dimensionally stable polymers having good thermal stability, is the simple and effective method to polymer gel electrolyte which have superior electrochemical properties and charge–discharge cycling stability even at high C-rate [32, 113]. PPC blended with different polymers such as poly(lactic acid) (PLLA) [114, 115], poly(3-hydroxybutrate) (PHB), triethyl citrate (TEC) [115] thermoplastic polyurethane (TPU) [113] and PVdF [113, 116, 117] for different applications such as mechanical applications [114] water purification, [115] battery electrolyte, [113, 116, 118] binder for electrodes in LIBs [117], etc. Electrospun PPC/PVdF binary blend [116] and PPC/PVdF/TPU tri-polymer blend [113] fibrous membrane activated with 1 M LiPF₆ in EC/DMC (1:1, v/v) are reported as polymer gel electrolyte for LIBs. As the PVdF has very stable polar fluorine atoms (-CF groups) in their backbone and high dielectric constant ($\epsilon = 8.4$) [7], blending of PPC with PVdF is beneficial in dissociating more lithium salt and conducting lithium ions in the polymer electrolytes, thereby improving the mobility and transference number of Li⁺-ions. In addition, the presence of PVdF in the polymer blend imparts the mechanical integrity, dimensional and thermal stability of the electrospun membranes which again make the membrane free-standing and easy to handle. Given the high crystallinity of PVdF, blending with the amorphous PPC is an effective way to reduce the crystallinity and facilitate Li⁺-ion transportation in the 3D polymeric framework. The effect of the ratio of PPC to PVdF (0 to 40 wt% PPC) [116] or PVdF/TPU blend (50:50 blend of PPC/PVdF with 12.5 wt% TPU) [113] on the properties of the highly porous membrane including morphology, porosity, liquid uptake capability, thermal stability, ionic conductivity and electrochemical behavior was systematically studied and reported. Table 8.5 summarizes the physical, thermal and electrochemical properties of these binary and ternary polymer blend electrolytes. It can be found that the incorporation of TPU in the PVdF/PPC blend has pronounced effect on ionic conductivity thereby Li⁺-ion transportation. The ternary blend shows higher ionic conductivity than PVdF/PPC, and it shows higher ionic conductivity at 25 °C [113] than the ionic conductivity of PVdF/PPC blend at higher temperature (30 °C) [116]. The evaluation of blend polymer gel electrolytes in Li/LiFePO₄ comprising 1 M LiPF₆ in EC/DMC (1:1, v/v) the PVdF/PPC blend electrolyte showed higher charge–discharge cycling stability and rate capability. The PVdF/PPC binary blend is having 20 wt% PPC delivered an initial discharge capacity of 156 mAh g⁻¹ (92% of theoretical capacity of LiFePO₄), which is about 4.5% higher than the pristine PVdF fibrous gel electrolyte. In comparison with Celgard[®], the PVdF or PVdF/PPC blend electrolyte delivered 2.5 to 7.6 higher capacities at a current density of 0.1 A g⁻¹ at room temperature. After 100 cycles, the capacity of pristine PVdF polymer gel electrolyte and Celgard[®] is faded

Table 8.5 Physical, thermal and electrochemical properties of these binary and ternary blend electrolytes

Sample	ΔH_m (J/g)	Crystallinity, X_c (%)	Porosity(%)	Electrolyte uptake(wt%)	Ionic conductivity (mS cm ⁻¹)	
Celgard			42	147	0.66	at 30 °C
PVdF/PPC (100:0)	21.4	20.4	77	422	2.11	
PVdF/PPC (90:10)	20	19.1	80	492	3.87	
PVdF/PPC (80:20)	16.3	15.6	85	501	4.05	
PVdF/PPC (70:30)	15.4	14.7	85.4	471	3.15	
PVdF/PPC(60:40)	11.7	11.2	87	450	2.43	
PVdF/TPU/PPC (9 wt%)	18.22	17.4	78.2	335	2.17	at 25 °C
PVdF/TPU/PPC (10 wt%)	17.67	16.9	87	379	3.27	
PVdF/TPU/PPC (11 wt%)	16.92	16.2	88	422	4.27	
PVdF/TPU/PPC (12 wt%)	14.55	13.9	85.5	449	5.32	
PVdF/TPU/PPC (13 wt%)	19.30	18.4	76	319	2.13	

to 93 and 90% of its initial capacity, but there was no capacity fade observed for PBDF/PPC binary blend (100th cycle capacity is 157 mAh g⁻¹). The rate capability studies at a current density of 0.1–2C showed the capacity is decreasing with current rate and when the current rate was reduced back to 0.2 C from 2C, after 25 cycles, a reversible capacity of 149 mAh g⁻¹ was obtained, showing the good rate capability of PVdF, PPC binary blend electrolyte [32, 116].

TPU is a polymer with good mechanical properties. It is commonly used to improve the elongation at break of other materials. It is a typical block polymer that contains two phases in the molecule [119]. The hard segment provides support function, so that it has good mechanical properties, such as tensile strength, wear resistance, high elasticity, etc. [120]. The soft segment can dissolve the cations in the lithium salts and facilitate the transportation of ions. When it is mixed with PVdF, the amino group (–NH) in its molecular chain can form hydrogen bonds with fluorine atoms, which makes the two polymers better compatible. The ternary blend consist of PVdF/PPC/TPU exhibits a three-dimensional network with randomly oriented nanofibers which enhance the porous structure (Fig. 8.10). When the concentration of ternary PVdF/PPC/TPU polymer blend increases from 9 to 13%, the initial charge–discharge capacity of the battery is increased to peak value from ~158.3 to

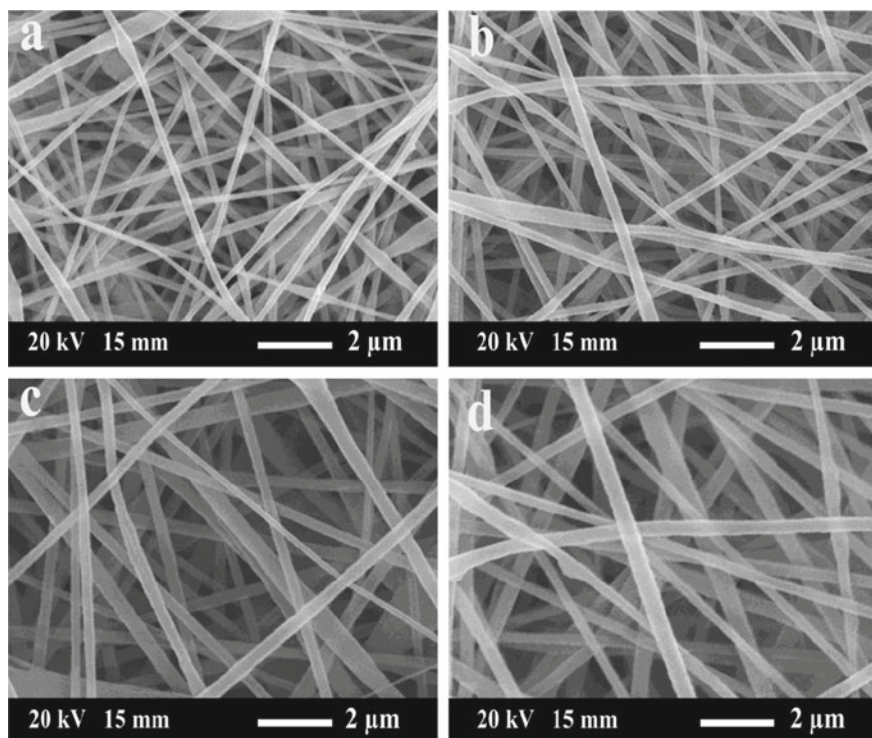


Fig. 8.10 Surface morphology of different concentration (wt%) of electrospun PVdF/TPU/PPC blend membranes **a** 9, **b** 10, **c** 11, **d** 13. Adapted and reproduced from Ref [113]. Copyright 2019 Springer

$\sim 165.8 \text{ mAh g}^{-1}$ with concentration, however concentration of the blend reached to 13% the peak value decayed to 157.5 mAh g^{-1} at a current density of 0.1 C. The charge–discharge capacity values are concurrent with ionic conductivity of the ternary blends electrolyte, and the entire tri-polymer blend delivered a capacity corresponding to more than 90% of the theoretical capacity of LiFePO_4 . After 50 continuous charge–discharge cycling, all the cell retained about 95–97% of its initial capacity suggesting the good cycling stability. Again, the rate capability studies on the PVdF/PPC/TPU-based blend polymer electrolyte PE (12 wt%) at different rates display good charge–discharge specific capacity and Coulombic efficiency at the current densities sweep between 0.1 and 1.0 C. At a current density of 1 C, the cell delivered a specific capacity of about 142 mAh g^{-1} , which corresponds to the 83.5% utilization of active material, after 200 cycle (Fig. 8.11) [113]. The capacity retention of these PVdF/PPC/TPU tri-polymer blends' polymer electrolyte is significantly higher than that of PVdF/PPC binary blends, which delivered a maximum capacity of about 105 mAh g^{-1} at 1 C-rate after 25 cycles [32]. The discharge capacities are the capacity retention percentages are 95.47%, 92.4%, 90.4% and 83.3%, respectively.

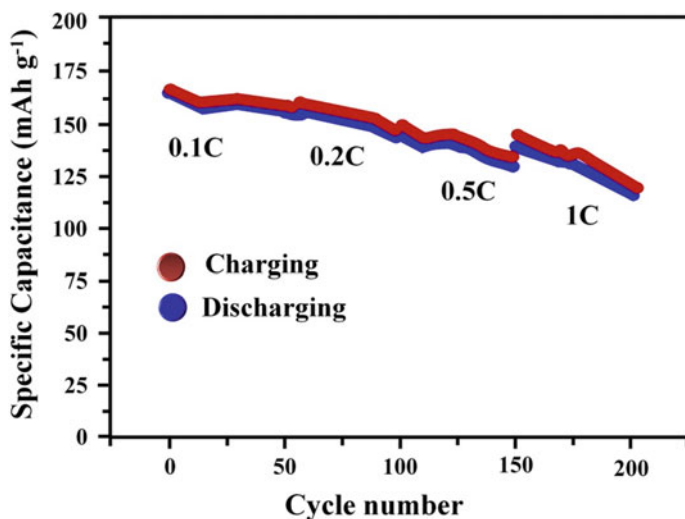


Fig. 8.11 Cycle performance and Coulombic efficiency diagram of the button battery with PVDF/TPU/PPC (12 wt%) based GPE at different rates. Adapted and reproduced from Ref [113]. Copyright 2019 Springer

The surface morphology of the electrospun PVdF and PVdF/PPC membranes with different weight ratios is shown in Fig. 8.12. The electrospun membranes result a three-dimensional network which formed by the random orientated nanofibers, which results in a porous structure. These porous structures result an increase the specific surface area that will results an enhanced electrolyte absorption and gelatinization efficiently as it soaked in electrolyte solution. The porous structure enables numerous ionic transport channels and that will provide a path way for fast Li^+ -ions transport. The AFD measured for the membranes is between 300 and 850 nm, and the AFD appears to decrease with increase in pPC to PVdF ratio.

Figure 8.13 shows the SEM images of the surface for the pristine PVdF and PVdF/PPC binary blend electrolyte having 20 wt% PPC membranes after the 100th charge/discharge cycle. The appearance of pristine PVdF and PVdF/PPC binary was well retained without appreciable signs of mechanical stress, maintaining the original three-dimensional network and hierarchically mesoporous structure. Specifically, the electrospun membranes with a porous structure readily relax the strain originated from mechanical stress during cycling. The electrospun membranes that offer ionic transport channels and provide a pathway for fast Li^+ ions transportation enable one to firmly maintain the shape of network and nanofibrous structure. The SEM images of the PVdF/PPC nanofibers show the AFD of about 700 nm, similar to the pristine electrospun membrane before cycling, as shown in Fig. 8.13b. By contrast, the VGE-100 nanofibers show volume expansion after cycling, which can be attributed to the presence of the swollen polymer chains [116].

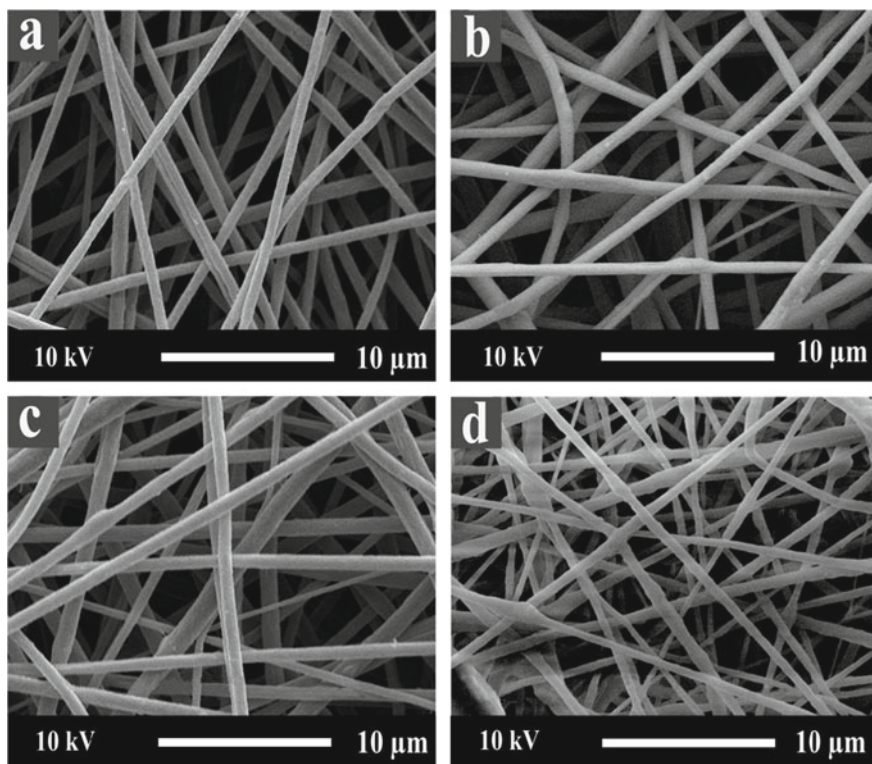


Fig. 8.12 SEM images on the surface morphology of the electrospun **a**. pristine PVdF, PVdF/PPC polymer blend membranes **b** 90:10; **c** 80:20; **d** 70:30. Adapted and reproduced from Ref. [116]. Copyright 2015 American Chemical Society

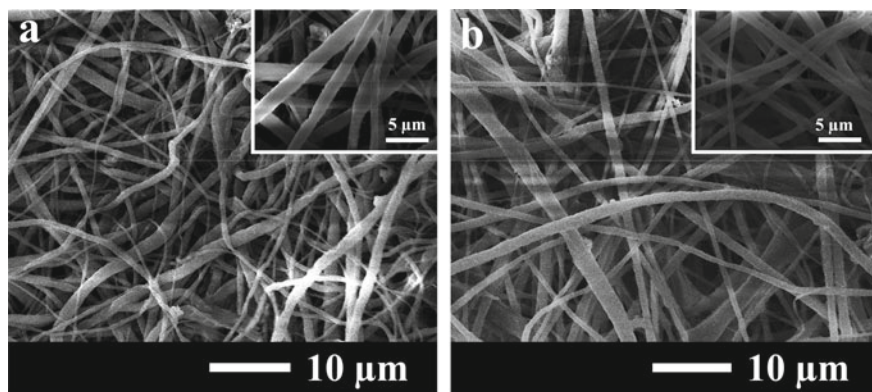


Fig. 8.13 Typical SEM images on the surface morphology of polymer membrane after activating with liquid electrolyte **a** VGE-100 (pristine PVdF) and **b** CGE-20 (PVdF/PPC (80:20)) after 100 cycles. Adapted and reproduced from Ref. [116]. Copyright 2015 American Chemical Society

The results show that our developed route has several distinct advantages: (1) The electrospun membranes present a three-dimensional network porous structure, which can greatly enlarge the specific surface area, promote the adsorption electrolyte and gelatinize efficiently; (2) the segregation of PVdF chains by polymeric chains of PPC can reduce the crystallization of PVdF-based polymers and increase the segmental mobility of the polymer, which benefit for the transport of lithium ions; (3) the formation of $\text{Li}^+\cdots(\delta^-)\text{F}-\text{C}(\delta^+)$ and $\text{PF}_6^-\cdots(\delta^+)\text{C}=\text{O}(\delta^-)$ complexes can separate the Li^+ and PF_6^- anions, which prevent the reconnection between Li^+ and PF_6^- anions simultaneously and create more free Li^+ (Fig. 8.14); thus, the ability of lithium-ion transference is improved. Therefore, the large surface area, well-developed microporous structure, sufficient electrolyte uptake, low crystallinity and appropriate porosity allow the electrospun PVdF/PPC polymer electrolyte to exhibit a significantly higher ionic conductivity and excellent electrochemical performances [116].

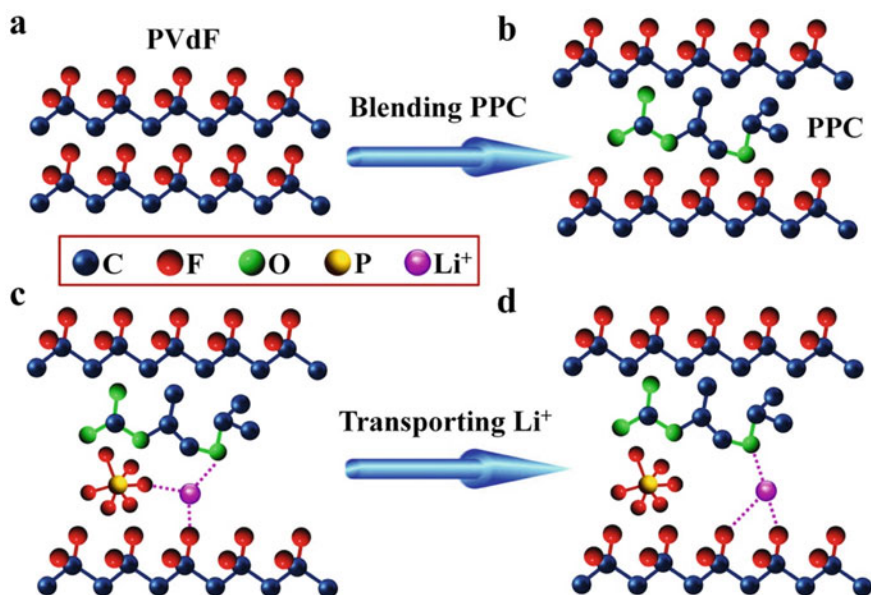


Fig. 8.14 Conceptual illustration of the polymer frameworks of **a** PVdF and **b** PVdF/PPC. Schematic illustration of main interaction forms between the ions and the polymer in the GPE. **c** Interaction of Li^+ between PF_6^- and the polymer chains; **d** transport of Li^+ -ions was associated with the ether linkages in the PPC and the fluorine atom in the PVdF. Adapted and reproduced from Ref. [116]. Copyright 2015 American Chemical Society

8.3 Conclusion

Electrospinning technique was widely used in energy storage devices such as batteries, supercapacitors. Electrospinning is one of the effective and attractive techniques for the preparation of fibrous polymer membranes having high surface area and porosity. Interconnected fibrous polymer electrolytes can be obtained by these techniques which exhibit high liquid electrolyte uptake leading to the high ionic conductivity. Different polymer electrolytes were used for the synthesis of electrolytes in which PVdF grabbed the attention as a favorable polymer matrix because of its high dielectric constant, high electrochemical stability, chemical compatibility, etc. The major drawback of this matrix is the hindrance of the migration of the doping salt since PVdF has a crystalline part offering low ionic conductivity. Blending other polymers along with PVdF can hinder the crystalline nature and pave an easy migration of lithium doping salt. PVdF blend polymer electrolytes prepared by this electrospinning technique show higher ionic conductivity.

References

1. Manthiram A (2017) An outlook on lithium ion battery technology. *ACS Cent Sci* 3:1063–1069. <https://doi.org/10.1021/acscentsci.7b00288>
2. Prize N History. In: Nobel media. <https://www.nobelpeaceprize.org/History>
3. Prasanth R, Shubha N, Hng HH, Srinivasan M (2013) Effect of nano-clay on ionic conductivity and electrochemical properties of poly(vinylidene fluoride) based nanocomposite porous polymer membranes and their application as polymer electrolyte in lithium ion batteries. *Eur Polym J* 49:307–318. <https://doi.org/10.1016/j.eurpolymj.2012.10.033>
4. Chiang C-Y, Jaipal Reddy M, Chu PP (2004) Nano-tube TiO₂ composite PVdF/LiPF₆ solid membranes. *Solid State Ionics* 175:631–635. <https://doi.org/10.1016/j.ssi.2003.12.039>
5. Wang Y-J, Kim D (2007) Crystallinity, morphology, mechanical properties and conductivity study of in situ formed PVdF/LiClO₄/TiO₂ nanocomposite polymer electrolytes. *Electrochim Acta* 52:3181–3189. <https://doi.org/10.1016/j.electacta.2006.09.070>
6. Gentili V, Panero S, Reale P, Scrosati B (2007) Composite gel-type polymer electrolytes for advanced, rechargeable lithium batteries. *J Power Sources* 170:185–190. <https://doi.org/10.1016/j.jpowsour.2007.04.008>
7. Prasanth R, Shubha N, Hng HH, Srinivasan M (2014) Effect of poly(ethylene oxide) on ionic conductivity and electrochemical properties of poly(vinylidene fluoride) based polymer gel electrolytes prepared by electrospinning for lithium ion batteries. *J Power Sources* 245:283–291. <https://doi.org/10.1016/j.jpowsour.2013.05.178>
8. Kim JR, Choi SW, Jo SM et al (2006) Characterization of electrospun PVdF fiber-based polymer electrolytes. *Chem Mater* 19:104–115. <https://doi.org/10.1021/cm060223+>
9. Shubha N, Prasanth R, Hoon HH, Srinivasan M (2013) Dual phase polymer gel electrolyte based on non-woven poly(vinylidene fluoride-co-hexafluoropropylene)-layered clay nanocomposite fibrous membranes for lithium ion batteries. *Mater Res Bull* 48:526–537. <https://doi.org/10.1016/j.materresbull.2012.11.002>
10. Raghavan P, Zhao X, Manuel J et al (2010) Electrochemical performance of electrospun poly(vinylidene fluoride-co-hexafluoropropylene)-based nanocomposite polymer electrolytes incorporating ceramic fillers and room temperature ionic liquid. *Electrochim Acta* 55:1347–1354. <https://doi.org/10.1016/j.electacta.2009.05.025>

11. Raghavan P, Zhao X, Kim JK et al (2008) Ionic conductivity and electrochemical properties of nanocomposite polymer electrolytes based on electrospun poly(vinylidene fluoride-co-hexafluoropropylene) with nano-sized ceramic fillers. *Electrochim Acta* 54:228–234. <https://doi.org/10.1016/j.electacta.2008.08.007>
12. Raghavan P, Zhao X, Choi H et al (2014) Electrochemical characterization of poly(vinylidene fluoride-co-hexafluoro propylene) based electrospun gel polymer electrolytes incorporating room temperature ionic liquids as green electrolytes for lithium batteries. *Solid State Ionics* 262:77–82. <https://doi.org/10.1016/j.ssi.2013.10.044>
13. Shubha N, Prasanth R, Hoon HH, Srinivasan M (2014) Plastic crystalline-semi crystalline polymer composite electrolyte based on non-woven poly(vinylidene fluoride-co-hexafluoropropylene) porous membranes for lithium ion batteries. *Electrochim Acta* 125:362–370. <https://doi.org/10.1016/j.electacta.2014.01.024>
14. Raghavan P, Choi J-W, Ahn J-H et al (2008) Novel electrospun poly(vinylidene fluoride-co-hexafluoropropylene)-in situ SiO₂ composite membrane-based polymer electrolyte for lithium batteries. *J Power Sources* 184:437–443. <https://doi.org/10.1016/j.jpowsour.2008.03.027>
15. Cheruvally G, Kim J-K, Choi J-W et al (2007) Electrospun polymer membrane activated with room temperature ionic liquid: novel polymer electrolytes for lithium batteries. *J Power Sources* 172:863–869. <https://doi.org/10.1016/j.jpowsour.2007.07.057>
16. Kim J-K, Cheruvally G, Li X et al (2008) Preparation and electrochemical characterization of electrospun, microporous membrane-based composite polymer electrolytes for lithium batteries. *J Power Sources* 178:815–820. <https://doi.org/10.1016/j.jpowsour.2007.08.063>
17. Shubha N, Prasanth R, Hng HH, Srinivasan M (2014) Study on effect of poly (ethylene oxide) addition and in-situ porosity generation on poly (vinylidene fluoride)-glass ceramic composite membranes for lithium polymer batteries. *J Power Sources* 267:48–57. <https://doi.org/10.1016/j.jpowsour.2014.05.074>
18. Kalyana Sundaram NT, Subramania A (2007) Nano-size LiAlO₂ ceramic filler incorporated porous PVDF-co-HFP electrolyte for lithium-ion battery applications. *Electrochim Acta* 52:4987–4993. <https://doi.org/10.1016/j.electacta.2007.01.066>
19. Jiang G, Maeda S, Yang H et al (2005) All solid-state lithium-polymer battery using poly(urethane acrylate)/nano-SiO₂ composite electrolytes. *J Power Sources* 141:143–148. <https://doi.org/10.1016/j.jpowsour.2004.09.004>
20. Raghavan P, Manuel J, Zhao X et al (2011) Preparation and electrochemical characterization of gel polymer electrolyte based on electrospun polyacrylonitrile nonwoven membranes for lithium batteries. *J Power Sources* 196:6742–6749. <https://doi.org/10.1016/j.jpowsour.2010.10.089>
21. Gopalan AI, Santhosh P, Manesh KM et al (2008) Development of electrospun PVdF-PAN membrane-based polymer electrolytes for lithium batteries. *J Memb Sci* 325:683–690. <https://doi.org/10.1016/j.memsci.2008.08.047>
22. Prasanth R, Aravindan V, Srinivasan M (2012) Novel polymer electrolyte based on cobweb electrospun multi component polymer blend of polyacrylonitrile/poly(methyl methacrylate)/polystyrene for lithium ion batteries—preparation and electrochemical characterization. *J Power Sources* 202:299–307. <https://doi.org/10.1016/j.jpowsour.2011.11.057>
23. Raghavan P, Zhao X, Shin C et al (2010) Preparation and electrochemical characterization of polymer electrolytes based on electrospun poly(vinylidene fluoride-co-hexafluoropropylene)/polyacrylonitrile blend/composite membranes for lithium batteries. *J Power Sources* 195:6088–6094. <https://doi.org/10.1016/j.jpowsour.2009.11.098>
24. Liao YH, Zhou DY, Rao MM et al (2009) Self-supported poly(methyl methacrylate-acrylonitrile-vinyl acetate)-based gel electrolyte for lithium ion battery. *J Power Sources* 189:139–144. <https://doi.org/10.1016/j.jpowsour.2008.10.027>
25. Lim D-H, Haridas AK, Figerez SP et al (2018) Tailor-made electrospun multilayer composite polymer electrolytes for high-performance lithium polymer batteries. *J Nanosci Nanotechnol* 18:6499–6505. <https://doi.org/10.1166/jnn.2018.15689>

26. Choi J-W, Cheruvally G, Kim Y-H et al (2007) Poly(ethylene oxide)-based polymer electrolyte incorporating room-temperature ionic liquid for lithium batteries. *Solid State Ionics* 178:1235–1241. <https://doi.org/10.1016/j.ssi.2007.06.006>
27. Caimi S, Klaue A, Wu H, Morbidelli M (2018) Effect of SiO₂ nanoparticles on the performance of PVdF-HFP/ionic liquid separator for lithium-ion batteries. *Nanomaterials* 8:926. <https://doi.org/10.3390/nano8110926>
28. Polu AR, Kumar R (2013) Effect of Al₂O₃ ceramic filler on peg-based composite polymer electrolytes for magnesium batteries. *Adv Mater Lett* 4:543–547. <https://doi.org/10.5185/aml.2012.9417>
29. Wu N, Cao Q, Wang X et al (2011) In situ ceramic fillers of electrospun thermoplastic polyurethane/poly(vinylidene fluoride) based gel polymer electrolytes for Li-ion batteries. *J Power Sources* 196:9751–9756. <https://doi.org/10.1016/j.jpowsour.2011.07.079>
30. Arya A, Sharma AL (2017) Polymer electrolytes for lithium ion batteries: a critical study. *Ionics (Kiel)* 23:497–540. <https://doi.org/10.1007/s11581-016-1908-6>
31. Stephan AM (2006) Review on gel polymer electrolytes for lithium batteries. *Eur Polym J* 42:21–42. <https://doi.org/10.1016/j.eurpolymj.2005.09.017>
32. Liu Y, Peng X, Cao Q et al (2017) Gel polymer electrolyte based on poly(vinylidene fluoride)/thermoplastic polyurethane/polyacrylonitrile by the electrospinning technique. *J Phys Chem C* 121:19140–19146. <https://doi.org/10.1021/acs.jpcc.7b03411>
33. Liang YZ, Cheng SC, Zhao JM et al (2013) Preparation and characterization of electrospun PVDF/PMMA composite fibrous membranes-based separator for lithium-ion batteries. *Adv Mater Res* 750–752:1914–1918. <https://doi.org/10.4028/www.scientific.net/amr.750-752.1914>
34. Manjuladevi R, Thamilselvan M, Selvasekarapandian S et al (2017) Mg-ion conducting blend polymer electrolyte based on poly(vinyl alcohol)-poly (acrylonitrile) with magnesium perchlorate. *Solid State Ionics* 308:90–100. <https://doi.org/10.1016/j.ssi.2017.06.002>
35. Zhou D, Zhou R, Chen C et al (2013) Non-volatile polymer electrolyte based on poly(propylene carbonate), Ionic liquid, and lithium perchlorate for electrochromic devices. *J Phys Chem B* 117:7783–7789. <https://doi.org/10.1021/jp4021678>
36. Ruan L, Yao X, Chang Y et al (2018) Properties and applications of the β phase poly(vinylidene fluoride). *Polymer (Guildf)* 10:1–27. <https://doi.org/10.3390/polym10030228>
37. Abrent S, Plestil J, Hlavata D et al (2001) Crystallinity and morphology of PVdF—HFP-based gel electrolytes. *Polymer* 42:1407–1416
38. Lewandowski A, Swiderska M (2013) Ionic liquids as electrolytes for Li-ion batteries—an overview of electrochemical studies. *Aviat Psychol Appl Hum Factors* 3:1–8. <https://doi.org/10.1016/j.jpowsour.2009.06.089>
39. Yu R, Bao JJ, Chen TT et al (2017) Solid polymer electrolyte based on thermoplastic polyurethane and its application in all-solid-state lithium ion batteries. *Solid State Ionics* 309:15–21. <https://doi.org/10.1016/j.ssi.2017.06.013>
40. In situ composite of nano SiO₂-P(VDF-HFP) porous polymer.pdf
41. Abraham KM, Alamgir M (1990) Li⁺-conductive solid polymer electrolytes with liquid-like conductivity. *J Electrochem Soc* 137:1657–1658. <https://doi.org/10.1149/1.2086749>
42. Wang F, Li L, Yang X et al (2018) Influence of additives in a PVDF-based solid polymer electrolyte on conductivity and Li-ion battery performance. *Sustain Energy Fuels* 2:492–498. <https://doi.org/10.1039/c7se00441a>
43. Rajendran S, Mahendran O, Kannan R (2002) Characterisation of [(1/2)x] PMMA ± x PVdF polymer blend electrolyte with Li ion q. *Fuel* 81:1077–1081
44. Kim CS, Oh SM (2002) Spectroscopic and electrochemical studies of PMMA-based gel polymer electrolytes modified with interpenetrating networks. *J Power Sources* 109:98–104. [https://doi.org/10.1016/S0378-7753\(02\)00055-1](https://doi.org/10.1016/S0378-7753(02)00055-1)
45. Lu H, Sun S (2018) Polyimide electrode materials for Li-ion batteries via dispersion-corrected density functional theory. *Comput Mater Sci* 146:119–125. <https://doi.org/10.1016/j.commat.2018.01.029>

46. Song JY, Wang YY, Wan CC (1999) Review of gel-type polymer electrolytes for lithium-ion batteries. *J Power Sources* 77:183–197. [https://doi.org/10.1016/S0378-7753\(98\)00193-1](https://doi.org/10.1016/S0378-7753(98)00193-1)
47. Lee H, Yanilmaz M, Toprakci O et al (2014) A review of recent developments in membrane separators for rechargeable lithium-ion batteries. *Energy Environ Sci* 7:3857–3886. <https://doi.org/10.1039/c4ee01432d>
48. Costa CM, Rodrigues HM, Gören A et al (2017) Preparation of poly(vinylidene fluoride) lithium-ion battery separators and their compatibilization with ionic liquid—a green solvent approach. *ChemistrySelect* 2:5394–5402. <https://doi.org/10.1002/slct.201701028>
49. Wang Z, Tang Z (2003) Characterization of the polymer electrolyte based on the blend of poly(vinylidene fluoride-co-hexafluoropropylene) and poly(vinyl pyrrolidone) for lithium ion battery. *Mater Chem Phys* 82:16–20. [https://doi.org/10.1016/S0254-0584\(03\)00241-4](https://doi.org/10.1016/S0254-0584(03)00241-4)
50. Choi J, Kim J, Cheruvally G et al (2006) Microporous poly (vinylidene fluoride-co-hexafluoropropylene) polymer electrolytes for lithium/sulfur cells. *J Ind Eng Chem* 12:939–949
51. Raghavan P, Zhao X, Manuel J et al (2010) Electrochemical studies on polymer electrolytes based on poly(vinylidene fluoride-co-hexafluoropropylene) membranes prepared by electrospinning and phase inversion—a comparative study. *Mater Res Bull* 45:362–366. <https://doi.org/10.1016/j.materresbull.2009.12.001>
52. Li X, Cheruvally G, Kim J-K et al (2007) Polymer electrolytes based on an electrospun poly(vinylidene fluoride-co-hexafluoropropylene) membrane for lithium batteries. *J Power Sources* 167:491–498. <https://doi.org/10.1016/j.jpowsour.2007.02.032>
53. Kim JR, Choi SW, Jo SM et al (2004) Electrospun PVdF-based fibrous polymer electrolytes for lithium ion polymer batteries. *Electrochim Acta* 50:69–75. <https://doi.org/10.1016/j.electacta.2004.07.014>
54. Choi SW, Kim JR, Jo SM et al (2005) Electrochemical and spectroscopic properties of electrospun PAN-based fibrous polymer electrolytes. *J Electrochem Soc* 152:A989. <https://doi.org/10.1149/1.1887166>
55. Sousa RE, Nunes-Pereira J, Ferreira JCC et al (2014) Microstructural variations of poly(vinylidene fluoride co-hexafluoropropylene) and their influence on the thermal, dielectric and piezoelectric properties. *Polym Test* 40:245–255. <https://doi.org/10.1016/j.polymertesting.2014.09.012>
56. Ahmad Z, Al-Awadi NA, Al-Sagheer F (2007) Morphology, thermal stability and visco-elastic properties of polystyrene-poly(vinyl chloride) blends. *Polym Degrad Stab* 92:1025–1033. <https://doi.org/10.1016/j.polymdegradstab.2007.02.016>
57. Nunes-Pereira J, Costa CM, Lanceros-Méndez S (2015) Polymer composites and blends for battery separators: state of the art, challenges and future trends. *J Power Sources* 281:378–398
58. Yee WA, Nguyen AC, Lee PS et al (2008) Stress-induced structural changes in electrospun polyvinylidene difluoride nanofibers collected using a modified rotating disk. *Polymer (Guildf)* 49:4196–4203. <https://doi.org/10.1016/j.polymer.2008.07.032>
59. Bansal D, Meyer B, Salomon M (2008) Gelled membranes for Li and Li-ion batteries prepared by electrospinning. *J Power Sources* 178:848–851. <https://doi.org/10.1016/j.jpowsour.2007.07.070>
60. Kim JF, Jung JT, Wang HH et al (2016) Microporous PVDF membranes via thermally induced phase separation (TIPS) and stretching methods. *J Memb Sci* 509:94–104. <https://doi.org/10.1016/j.memsci.2016.02.050>
61. Ribeiro C, Costa CM, Correia DM et al (2018) Electroactive poly(vinylidene fluoride)-based structures for advanced applications. *Nat Protoc* 13:681–704. <https://doi.org/10.1038/nprot.2017.157>
62. Martins P, Lopes AC, Lanceros-Mendez S (2014) Electroactive phases of poly(vinylidene fluoride): determination, processing and applications. *Prog Polym Sci* 39:683–706. <https://doi.org/10.1016/j.progpolymsci.2013.07.006>
63. Edmonds EA, Acharya UR, Bonjour E, et al (2007) Founding editor, 193. [https://doi.org/10.1016/S0950-7051\(18\)30220-X](https://doi.org/10.1016/S0950-7051(18)30220-X)

64. Du Pasquier A, Warren PC, Culver D et al (2000) Plastic PVDF-HFP electrolyte laminates prepared by a phase-inversion process. *Solid State Ionics* 135:249–257. [https://doi.org/10.1016/S0167-2738\(00\)00371-4](https://doi.org/10.1016/S0167-2738(00)00371-4)
65. Li ZH, Xiao QZ, Zhang P et al (2008) Porous nanocomposite polymer electrolyte prepared by a non-solvent induced phase separation process. *Funct Mater Lett* 1:139–143. <https://doi.org/10.1142/S1793604708000253>
66. Costa CM, Silva MM, Lanceros-Méndez S (2013) Battery separators based on vinylidene fluoride (VDF) polymers and copolymers for lithium ion battery applications. *RSC Adv* 3:11404–11417. <https://doi.org/10.1039/c3ra40732b>
67. Sousa RE, Ferreira JCC, Costa CM et al (2015) Tailoring poly(vinylidene fluoride-co-chlorotrifluoroethylene) microstructure and physicochemical properties by exploring its binary phase diagram with dimethylformamide. *J Polym Sci, Part B: Polym Phys* 53:761–773. <https://doi.org/10.1002/polb.23692>
68. Costa CM, Rodrigues LC, Sencadas V et al (2012) Effect of degree of porosity on the properties of poly(vinylidene fluoride–trifluorethylene) for Li-ion battery separators. *J Memb Sci* 407–408:193–201. <https://doi.org/10.1016/j.memsci.2012.03.044>
69. Bohne O, Frand G, Rezrazi M et al (1993) Fast ion transport in new lithium electrolytes gelled with PMMA. 1. Influence of polymer concentration. *Solid State Ionics* 66:97–104. [https://doi.org/10.1016/0167-2738\(93\)90032-X](https://doi.org/10.1016/0167-2738(93)90032-X)
70. Appetecchi GB, Croce F, Scrosati B (1995) Kinetics and stability of the lithium electrode in poly(methylmethacrylate)-based gel electrolytes. *Electrochim Acta* 40:991–997. [https://doi.org/10.1016/0013-4686\(94\)00345-2](https://doi.org/10.1016/0013-4686(94)00345-2)
71. Rhoo H-J, Kim H-T, Park J-K, Hwang T-S (1997) Ionic conduction in plasticized PVC/PMMA blend polymer electrolytes. *Electrochim Acta* 42:1571–1579. [https://doi.org/10.1016/S0013-4686\(96\)00318-0](https://doi.org/10.1016/S0013-4686(96)00318-0)
72. Tatsuma T, Taguchi M, Oyama N (2001) Inhibition effect of covalently cross-linked gel electrolytes on lithium dendrite formation. *Electrochim Acta* 46:1201–1205. [https://doi.org/10.1016/S0013-4686\(00\)00706-4](https://doi.org/10.1016/S0013-4686(00)00706-4)
73. Gray FM, MacCallum JR, Vincent CA (1986) Poly(ethylene oxide)—LiCF₃SO₃—polystyrene electrolyte systems. *Solid State Ionics* 18–19:282–286. [https://doi.org/10.1016/0167-2738\(86\)90127-X](https://doi.org/10.1016/0167-2738(86)90127-X)
74. Mahant YP, Kondawar SB, Bhute M, Nandanwar DV (2015) Electrospun poly (vinylidene fluoride)/poly (methyl methacrylate) composite nanofibers polymer electrolyte for batteries. *Procedia Mater Sci* 10:595–602. <https://doi.org/10.1016/j.mspro.2015.06.011>
75. Mahant YP, Kondawar SB, Nandanwar DV, Koinkar P (2018) Poly(methyl methacrylate) reinforced poly(vinylidene fluoride) composites electrospun nanofibrous polymer electrolytes as potential separator for lithium ion batteries. *Mater Renew Sustain Energy* 7:1–9. <https://doi.org/10.1007/s40243-018-0115-y>
76. Ding Y, Zhang P, Long Z et al (2009) The ionic conductivity and mechanical property of electrospun P(VdF-HFP)/PMMA membranes for lithium ion batteries. *J Memb Sci* 329:56–59. <https://doi.org/10.1016/j.memsci.2008.12.024>
77. Tominaga Y, Nanthana V, Tohyama D (2012) Ionic conduction in poly(ethylene carbonate)-based rubbery electrolytes including lithium salts. *Polym J* 44:1155–1158. <https://doi.org/10.1038/pj.2012.97>
78. Deng F, Wang X, He D et al (2015) Microporous polymer electrolyte based on PVDF/PEO star polymer blends for lithium ion batteries. *J Memb Sci* 491:82–89. <https://doi.org/10.1016/j.memsci.2015.05.021>
79. Polu AR, Rhee H-W (2015) Nanocomposite solid polymer electrolytes based on poly(ethylene oxide)/POSS-PEG (n = 13.3) hybrid nanoparticles for lithium ion batteries. *J Ind Eng Chem* 31:323–329. <https://doi.org/10.1016/j.jiec.2015.07.005>
80. Konnik OV, Shul'gin VF, Bekirova ZZ et al (2014) Coordination compounds of dysprosium(III) with 3-methyl-1-phenyl-4-formylpyrazol-5-one diacyldihydrazones. *Russ J Inorg Chem* 59:1237–1243. <https://doi.org/10.1134/S0036023614110126>

81. Appetecchi GB, Croce F, Hassoun J et al (2003) Hot-pressed, dry, composite, PEO-based electrolyte membranes: I. Ionic conductivity characterization. *J Power Sources* 114:105–112. [https://doi.org/10.1016/S0378-7753\(02\)00543-8](https://doi.org/10.1016/S0378-7753(02)00543-8)
82. Shin JH, Lim YT, Kim KW et al (2002) Effect of ball milling on structural and electrochemical properties of (PEO)_nLiX (LiX = LiCF₃SO₃ and LiBF₄) polymer electrolytes. *J Power Sources* 107:103–109. [https://doi.org/10.1016/S0378-7753\(01\)00990-9](https://doi.org/10.1016/S0378-7753(01)00990-9)
83. Ramrakhiani M, Nogriya V (2012) Synthesis and characterization of zinc sulfide nanocrystals and zinc sulfide/polyvinyl alcohol nanocomposites for luminescence applications. *Polym Process Charact* 394:109–138. <https://doi.org/10.1201/b13105>
84. Shi J, Yang Y, Shao H (2018) Co-polymerization and blending based PEO/PMMA/P(VDF-HFP) gel polymer electrolyte for rechargeable lithium metal batteries. *J Memb Sci* 547:1–10. <https://doi.org/10.1016/j.memsci.2017.10.033>
85. Nagarajan S, Santhosh P, Sankarasubramanian M et al (2005) UV–vis spectroscopy for following the kinetics of homogeneous polymerization of diphenylamine in p-toluene sulphonic acid. *Spectrochim Acta Part A Mol Biomol Spectrosc* 62:420–430. <https://doi.org/10.1016/j.saa.2005.01.010>
86. Wen T-C, Chen J-B, Gopalan A (2002) Soluble and methane sulfonic acid doped poly(diphenylamine)—synthesis and characterization. *Mater Lett* 57:280–290. [https://doi.org/10.1016/S0167-577X\(02\)00779-6](https://doi.org/10.1016/S0167-577X(02)00779-6)
87. Orlov AV, Ozkan SZ, Karpacheva GP (2006) Oxidative polymerization of diphenylamine: a mechanistic study. *Polym Sci Ser B* 48:11–17. <https://doi.org/10.1134/S1560090406010039>
88. Santhosh P, Sankarasubramanian M, Thanneermalai M et al (2004) Electrochemical, spectroelectrochemical and spectroscopic evidences for copolymer formation between diphenylamine and m-toluidine. *Mater Chem Phys* 85:316–328. <https://doi.org/10.1016/j.matchemphys.2004.01.021>
89. Hua F, Ruckenstein E (2003) Water-soluble conducting poly (ethylene oxide)—grafted poly-diphenylamine synthesis through a “Graft Onto” process. *Macromolecules* 36:9971–9978. <https://doi.org/10.1021/ma030431c>
90. Gopalan AI, Lee K-P, Manesh KM, Santhosh P (2008) Poly(vinylidene fluoride)—poly-diphenylamine composite electrospun membrane as high-performance polymer electrolyte for lithium batteries. *J Memb Sci* 318:422–428. <https://doi.org/10.1016/j.memsci.2008.03.007>
91. Choi SW, Jo SM, Lee WS, Kim YR (2003) An electrospun poly(vinylidene fluoride) nanofibrous membrane and its battery applications. *Adv Mater* 15:2027–2032. <https://doi.org/10.1002/adma.200304617>
92. Chiang C-Y, Shen YJ, Reddy MJ, Chu PP (2003) Complexation of poly(vinylidene fluoride): LiPF₆ solid polymer electrolyte with enhanced ion conduction in ‘wet’ form. *J Power Sources* 123:222–229. [https://doi.org/10.1016/S0378-7753\(03\)00514-7](https://doi.org/10.1016/S0378-7753(03)00514-7)
93. Panero S, Ciuffa F, D’Epifano A, Scrosati B (2003) New concepts for the development of lithium and proton conducting membranes. *Electrochim Acta* 48:2009–2014. [https://doi.org/10.1016/S0013-4686\(03\)00179-8](https://doi.org/10.1016/S0013-4686(03)00179-8)
94. Choi S-S, Lee YS, Joo CW et al (2004) Electrospun PVDF nanofiber web as polymer electrolyte or separator. *Electrochim Acta* 50:339–343. <https://doi.org/10.1016/j.electacta.2004.03.057>
95. Choe HS, Giaccai J, Alamgir M, Abraham KM (1995) Preparation and characterization of poly(vinyl sulfone)- and poly(vinylidene fluoride)-based electrolytes. *Electrochim Acta* 40:2289–2293. [https://doi.org/10.1016/0013-4686\(95\)00180-M](https://doi.org/10.1016/0013-4686(95)00180-M)
96. Gozdz AS, Schmutz CN, Tarascon J-M, Warren PC (1995) Method of making an electrolyte activatable lithium-ion rechargeable battery cell
97. Quartarone E, Brusa M, Mustarelli P et al (1998) Preparation and characterization of fluorinated hybrid electrolytes. *Electrochim Acta* 44:677–681. [https://doi.org/10.1016/S0013-4686\(98\)00182-0](https://doi.org/10.1016/S0013-4686(98)00182-0)
98. Stolarska M, Niedzicki L, Borkowska R et al (2007) Structure, transport properties and interfacial stability of PVdF/HFP electrolytes containing modified inorganic filler. *Electrochim Acta* 53:1512–1517. <https://doi.org/10.1016/j.electacta.2007.05.079>

99. Dai H, Zawodzinski TA (1998) The dependence of lithium transference numbers on temperature, salt concentration and anion type in poly(vinylidene fluoride)–hexafluoropropylene copolymer-based gel electrolytes (Presented at the Electrochemical Society Symposium: Processes in Polymers and Polymers). *J Electroanal Chem* 459:111–119. [https://doi.org/10.1016/S0022-0728\(98\)00373-8](https://doi.org/10.1016/S0022-0728(98)00373-8)
100. Kataoka H, Saito Y, Miyazaki Y, Deki S (2002) Ionic mobilities of PVDF-based polymer gel electrolytes as studied by direct current NMR. *Solid State Ionics* 152–153:175–179. [https://doi.org/10.1016/S0167-2738\(02\)00297-7](https://doi.org/10.1016/S0167-2738(02)00297-7)
101. Ramesh S, Winie T, Arof AK (2007) Investigation of mechanical properties of polyvinyl chloride–polyethylene oxide (PVC–PEO) based polymer electrolytes for lithium polymer cells. *Eur Polym J* 43:1963–1968. <https://doi.org/10.1016/j.eurpolymj.2007.02.006>
102. Rajendran S, Shanker Babu R, Sivakumar P (2008) Investigations on PVC/PAN composite polymer electrolytes. *J Memb Sci* 315:67–73. <https://doi.org/10.1016/j.memsci.2008.02.007>
103. Rajendran S, Sivakumar P, Shanker R (2007) Studies on the salt concentration of a PVdF–PVC based polymer blend electrolyte. *J Power Sources* 164:815–821. <https://doi.org/10.1016/j.jpowsour.2006.09.011>
104. Vickraman P, Ramamurthy S (2006) A study on the blending effect of PVDF in the ionic transport mechanism of plasticized PVC–LiBF₄ polymer electrolyte. *Mater Lett* 60:3431–3436. <https://doi.org/10.1016/j.matlet.2006.03.028>
105. Muniyandi N, Kalaiselvi N, Periyasamy P et al (2001) Optimisation of PVdF-based polymer electrolytes. *J Power Sources* 96:14–19. [https://doi.org/10.1016/S0378-7753\(01\)00562-6](https://doi.org/10.1016/S0378-7753(01)00562-6)
106. Zhong Z, Cao Q, Jing B et al (2012) Novel electrospun PAN – PVC composite fibrous membranes as polymer electrolytes for polymer lithium-ion batteries. *Ionics* 18:853–859. <https://doi.org/10.1007/s11581-012-0682-3>
107. Zhong Z, Cao Q, Jing B et al (2012) Electrospun PVdF–PVC nanofibrous polymer electrolytes for polymer lithium-ion batteries. *Mater Sci Eng B* 177:86–91. <https://doi.org/10.1016/j.mseb.2011.09.008>
108. Zeng S, Wang S, Xiao M et al (2011) Preparation and properties of biodegradable blend containing poly(propylene carbonate) and starch acetate with different degrees of substitution. *Carbohydr Polym* 86:1260–1265. <https://doi.org/10.1016/j.carbpol.2011.06.023>
109. Du L, Qu B, Meng Y, Zhu Q (2006) Structural characterization and thermal and mechanical properties of poly(propylene carbonate)/MgAl-LDH exfoliation nanocomposite via solution intercalation. *Compos Sci Technol* 66:913–918. <https://doi.org/10.1016/j.compscitech.2005.08.012>
110. Sugimoto H, Inoue S (2004) Copolymerization of carbon dioxide and epoxide. *J Polym Sci Part A Polym Chem* 42:5561–5573. <https://doi.org/10.1002/pola.20319>
111. Li XH, Meng YZ, Wang SJ et al (2004) Completely biodegradable composites of poly(propylene carbonate) and short, lignocellulose fiber *Hildegardia populifolia*. *J Polym Sci Part B Polym Phys* 42:666–675. <https://doi.org/10.1002/polb.10761>
112. Shi X, Gan Z (2007) Preparation and characterization of poly(propylene carbonate)/montmorillonite nanocomposites by solution intercalation. *Eur Polym J* 43:4852–4858. <https://doi.org/10.1016/j.eurpolymj.2007.09.024>
113. Xu J, Liu Y, Cao Q et al (2019) A high-performance gel polymer electrolyte based on poly(vinylidene fluoride)/thermoplastic polyurethane/poly(propylene carbonate) for lithium-ion batteries. *J Chem Sci* 131:1–10. <https://doi.org/10.1007/s12039-019-1627-4>
114. Gao J, Bai H, Zhang Q et al (2012) Effect of homopolymer poly(vinyl acetate) on compatibility and mechanical properties of poly(propylene carbonate)/poly(lactic acid) blends. *Express Polym Lett* 6:860–870. <https://doi.org/10.3144/expresspolymlett.2012.92>
115. El-Hadi AM, Alamri HR (2018) The new generation from biomembrane with green technologies for wastewater treatment. *Polymers (Basel)* 10:1174. <https://doi.org/10.3390/polym10101174>
116. Huang X, Zeng S, Liu J et al (2015) High-performance electrospun poly(vinylidene fluoride)/poly(propylene carbonate) gel polymer electrolyte for lithium-ion batteries. *J Phys Chem C* 119:27882–27891. <https://doi.org/10.1021/acs.jpcc.5b09130>

117. Zheng M, Fu X, Wang Y et al (2018) Poly(vinylidene fluoride)-based blends as new binders for lithium-ion batteries. *ChemElectroChem* 5:2288–2294. <https://doi.org/10.1002/celec.201800553>
118. Li H, Zhang H, Liang Z-Y et al (2014) Preparation and properties of poly (vinylidene fluoride)/poly(dimethylsiloxane) graft (poly(propylene oxide)-block-poly(ethylene oxide)) blend porous separators and corresponding electrolytes. *Electrochim Acta* 116:413–420. <https://doi.org/10.1016/j.electacta.2013.11.076>
119. van Heumen JD, Stevens JR (1995) The role of lithium salts in the conductivity and phase morphology of a thermoplastic polyurethane. *Macromolecules* 28:4268–4277. <https://doi.org/10.1021/ma00116a030>
120. Wu N, Jing B, Cao Q, Wang X, Kuang H, Wang Q (2010) A novel electrospun TPU/PVdF porous fibrous polymer electrolyte for lithium ion batteries. *J Appl Polym Sci* 116:2658–2667. <https://doi.org/10.1002/app>